AgriEngineering

MDPI

Article

Integration of IoT Technologies and High-Performance Phenotyping for Climate Control in Greenhouses and Mitigation of Water Deficit: A Study of High-Andean Oat

Edwin Villagran [1,*], Gabriela Toro-Tobón [2], Fabián Andrés Velázquez [2] and German A. Estrada-Bonilla [2]

[1] Corporación Colombiana de Investigación Agropecuaria—Agrosavia, Sede Central, Km 14, Vía Mosquera-Bogotá, Mosquera 250040, Colombia
[2] Corporación Colombiana de Investigación Agropecuaria—Agrosavia, Centro de Investigación Tibaitata, Km 14, Vía Mosquera-Bogotá, Mosquera 250040, Colombia; gtorot@agrosavia.co (G.T.-T.); favelasquez@agrosavia.co (F.A.V.); gaestrada@agrosavia.co (G.A.E.-B.)
* Correspondence: evillagran@agrosavia.co; Tel.: +57-1-4227-300 (ext. 1239)

Abstract: Climate change has intensified droughts, severely impacting crops like oats and highlighting the need for effective adaptation strategies. In this context, the implementation of IoT-based climate control systems in greenhouses emerges as a promising solution for optimizing microclimates. These systems allow for the precise monitoring and adjustment of critical variables such as temperature, humidity, vapor pressure deficit (VPD), and photosynthetically active radiation (PAR), ensuring optimal conditions for crop growth. During the experiment, the average daytime temperature was 22.6 °C and the nighttime temperature was 15.7 °C. The average relative humidity was 60%, with a VPD of 0.46 kPa during the day and 1.26 kPa at night, while the PAR reached an average of 267 µmol m^{-2} s^{-1}. Additionally, the use of high-throughput gravimetric phenotyping platforms enabled precise data collection on the plant–soil–atmosphere relationship, providing exhaustive control over water balance and irrigation. This facilitated the evaluation of the physiological response of plants to abiotic stress. Inoculation with microbial consortia (PGPB) was used as a tool to mitigate water stress. In this 69-day study, irrigation was suspended in specific treatments to simulate drought, and it was observed that inoculated plants maintained chlorophyll b and carotenoid levels akin to those of irrigated plants, indicating greater tolerance to water deficit. These plants also exhibited greater efficiency in dissipating light energy and rapid recovery after rehydration. The results underscore the potential of combining IoT monitoring technologies, advanced phenotyping platforms, and microbial consortia to enhance crop resilience to climate change.

Keywords: big data; gravimetric lysimeters; greenhouse microclimate; plant growth-promoting bacteria; sustainable agriculture; water resource management

check for updates

Citation: Villagran, E.; Toro-Tobón, G.; Velázquez, F.A.; Estrada-Bonilla, G.A. Integration of IoT Technologies and High-Performance Phenotyping for Climate Control in Greenhouses and Mitigation of Water Deficit: A Study of High-Andean Oat. *AgriEngineering* **2024**, *6*, 4011–4040. https://doi.org/10.3390/agriengineering6040227

Academic Editor: Murali Krishna Gumma

Received: 16 August 2024
Revised: 30 September 2024
Accepted: 22 October 2024
Published: 29 October 2024

Copyright: © 2024 by the authors. Licensee MDPI, Basel, Switzerland. This article is an open access article distributed under the terms and conditions of the Creative Commons Attribution (CC BY) license (https://creativecommons.org/licenses/by/4.0/).

1. Introduction

The gradual rise in the Earth's average temperature, driven by anthropogenic climate change, is causing significant alterations in global climate patterns. These changes are characterized by more frequent and intense climate variability, extreme seasonal temperatures, and an increase in the intensity of tropical storms [1–3]. Additionally, precipitation patterns are becoming more erratic and unpredictable, both in terms of timing and spatial distribution [4]. These shifts are leading to prolonged droughts, and when combined with high temperatures, they place substantial stress on a wide range of crops [5]. This stress severely impacts agricultural productivity, reducing plants' ability to grow and produce efficiently [6].

This type of abiotic stress can lead to crop production losses ranging from 50% to 70% globally [7]. Drought's impact on plants is evident at the morphological, physiological, and biochemical levels, manifesting in reduced growth, impaired root development, and

alterations in photosynthesis and transpiration processes [8]. Additionally, drought stress can compromise the integrity of cell membranes, disrupt protein synthesis, and alter hormonal balances, resulting in overall declines in plant health and productivity [9]. In cereals such as forage oats (*Avena sativa*), drought can sharply reduce biomass production, flower fertility, grain filling, and photosynthetic rates [10]. Moreover, drought can degrade forage quality by impacting its nutritional content and digestibility while also stunting root growth, thus limiting the plant's capacity to absorb water and nutrients [11]. These combined effects diminish water use efficiency and reduce the plant's resilience to adverse environmental conditions.

To tackle these challenges, the development of validated mitigation strategies through the use of advanced technologies is essential [12]. In crop-focused experimental greenhouses, the integration of Internet of Things (IoT) technologies for climate monitoring and control offers a promising approach [13,14]. These technologies enable accurate, real-time monitoring and management of environmental conditions, significantly improving water use efficiency and optimizing growth conditions [15]. Furthermore, IoT technology plays a pivotal role in greenhouse agriculture by integrating various advanced technologies, including smart machinery, actuators, sensors, phenotyping platforms, big data analytics, artificial intelligence, and satellite systems. This technological convergence enables precise monitoring and control of environmental parameters, optimizing crop growth and enhancing resource management efficiency [16,17].

In greenhouse soilless cucumber cultivation, the implementation of an IoT platform led to an increase in crop yield and quality, alongside a 28% improvement in water use efficiency and a reduction in energy consumption [17]. Similarly, an experimental system in a small-scale greenhouse demonstrated cost-effectiveness by incorporating photovoltaic panels and batteries, reducing operational costs while ensuring functionality during nighttime and cloudy conditions [18]. These automated systems monitor variables such as temperature, humidity, and light, adjusting environmental conditions to optimize plant growth. Furthermore, drip irrigation is managed automatically based on soil moisture levels, further enhancing precision and water use efficiency [19].

Another noteworthy example involves the use of customized wireless sensors to evaluate microclimates in tropical greenhouses. These studies validated key parameters, such as vapor pressure deficit, which reached a maximum of 5.1 kPa in polycarbonate greenhouses and 3.81 kPa in mesh-covered greenhouses, optimizing conditions for tomato growth [20]. Additionally, real-time data collection through IoT systems enabled the automatic activation of fog-based cooling systems when temperatures exceeded 30 °C or humidity dropped below 80%, achieving a temperature decrease of 6.25 °C and a 28.06% increase in relative humidity [21]. This technology has also improved microclimate management through the integration of Zigbee and LoRa wireless communication systems, which are well-suited for both short- and long-range greenhouse applications [22]. These advancements contribute to optimizing agricultural yield while reducing energy consumption.

In the transition from "Agriculture 1.0" to "Agriculture 4.0," phenotyping has progressed from manual measurements using rulers and basic instruments to advanced, multi-scale, high-precision, and high throughput monitoring modes [23]. Gravimetric high-throughput phenotyping platforms are transforming agricultural research by providing accurate assessments of crop phenotypic traits [24,25]. These platforms incorporate sophisticated weighing and sensing technologies to accurately measure plant water uptake and loss, enabling detailed analysis of water use efficiency and responses to water stress. Equipped with automated data acquisition and analysis systems, they continuously monitor key parameters such as biomass, transpiration rate, and water content in both soil and plants [26,27]. By deploying these tools in greenhouses, researchers can monitor the real-time effects of different environmental conditions and management strategies, promoting the development of more resilient, water-efficient crops and optimizing both yield and sustainability in water-stressed environments [28].

One of the key platforms in high-throughput phenotyping is the PlantArray by Plant-Ditech, which has proven to be an essential tool for the real-time monitoring of plant physiological responses under various environmental stress conditions. For instance, in a study by Illouz-Eliaz et al. [29], the platform was used to evaluate how tomato plants with mutations in gibberellin (GA) receptors exhibited improved water retention and reduced transpiration rates during drought stress. PlantArray enabled the detailed monitoring of the plants' water dynamics. Similarly, Sacco Botto et al. [30] used phenotyping platforms to show how tomato plants infected with begomovirus demonstrated increased drought stress tolerance, using recovery times and responses to water stress as key metrics. In Uni et al. [31], PlantArray tracked the water balance in *Acacia* species, revealing specific stomatal responses under controlled vapor pressure deficit (VPD) conditions, providing essential insights for species-specific water management. Additionally, Jaramillo Roman et al. [32] used the platform to evaluate salt tolerance in quinoa varieties, measuring stomatal conductance and transpiration across different saline concentrations. The phenotypic data enabled the identification of "conservative" and "acquisitive" water use strategies, which were crucial for understanding salt stress tolerance. When combined with mechanistic models such as the LINTUL crop model, these data provided valuable insights into stress management and potential breeding targets for quinoa under saline conditions.

Plant growth-promoting bacteria (PGPB) represent a promising biotechnological tool mitigating water stress in crops [33]. These beneficial bacteria, present in the rhizosphere and endosphere of plants, enhance plant resilience to adverse conditions such as drought by promoting root growth and health [34]. PGPB can increase the availability of essential nutrients, produce phytohormones that stimulate plant growth, and improve plants' ability to absorb water [35,36]. Additionally, these bacteria can induce the production of osmoprotective compounds in plants, allowing them to maintain cellular function and reduce the negative impact of water stress [37]. In research greenhouses, the application of PGPB enables the evaluation of their efficacy under controlled conditions, yielding valuable data on how these bacteria enhance drought tolerance in crops of agricultural significance. Integrating PGPB with advanced climate monitoring and control technologies optimizes water management, enhancing both the sustainability and productivity of crops under the challenges posed by climate change scenarios [38,39].

The main objective of this article is to evaluate the integration of IoT technologies and high-throughput gravimetric phenotyping platforms for monitoring and climate control in greenhouses, aiming to develop tools to mitigate water stress in crops. The specific objectives are: (1) to analyze how the implementation of IoT systems improves data collection efficiency and optimizes growth conditions in experimental greenhouses; (2) to use high-throughput gravimetric phenotyping platforms to accurately monitor the water balance in the plant–soil–atmosphere system; (3) to investigate the impact of using PGPB on the resistance of oat crops to water stress; and (4) to provide practical recommendations for the adoption of these technologies in modern agriculture, highlighting their potential to increase crop resilience to the adverse effects of climate change.

To address these challenges, advanced climate monitoring and control methods were implemented. The use of Internet of Things (IoT)-based technologies enabled real-time monitoring of environmental conditions in greenhouses, automatically adjusting key variables such as temperature, humidity, vapor pressure deficit (VPD), and photosynthetically active radiation (PAR). Additionally, high-throughput gravimetric phenotyping platforms were employed to accurately and continuously measure the water balance in plants, allowing for a detailed assessment of plant physiological responses to water stress. These approaches were complemented by rigorous statistical analyses to validate the results, processed using tools such as Excel and the R programming language, ensuring a robust and reliable interpretation of the data. The novelty of this study lies in the integration of these advanced technologies, applied to oat cultivation under water stress conditions in Colombian greenhouses. This combination not only allowed for precise microclimate monitoring and a comprehensive evaluation of plant physiological responses, but also

introduced the use of PGPB consortia as a biotechnological tool to mitigate water stress. The main contribution of this work is the simultaneous implementation of these technological and biotechnological tools in a controlled experiment, providing comprehensive data to optimize water management and evaluate the effectiveness of microbial consortia, which has not been explored as thoroughly in this context.

The remainder of this article is structured as follows: Section 2 describes the materials and methods used in the experimental setup, including the implementation of IoT-based climate control systems, gravimetric phenotyping platforms, and microbial consortium inoculation. Section 3 presents and discusses the results, offering detailed analyses of environmental data, plant physiological responses, and the efficacy of PGPB consortia under drought stress conditions. This section also includes a discussion of the implications of these results, comparing them with previous studies and evaluating their significance for improving crop resilience. Section 4 outlines practical applications of the study's relevant findings. Finally, Section 5 provides conclusions and practical recommendations for the adoption of these technologies in modern agriculture, along with suggestions for future research.

2. Materials and Methods

The methodology of this study was designed to evaluate the impact of advanced technologies, such as high-throughput gravimetric phenotyping platforms and IoT-based climate control systems, on the physiological response of oat crops under water stress. Experimental greenhouses were employed, where key variables such as temperature, humidity, and vapor pressure deficit (VPD) were monitored and adjusted to maintain an optimal microclimate for crop growth. Additionally, PGPB consortia were integrated to investigate their capacity to mitigate the effects of water stress. The data collection tools included automated climate monitoring systems, rigorous statistical analyses, and mechanistic models to evaluate plant responses to stress, ensuring a robust and reliable interpretation of the results.

2.1. Experimental Environment and Procedure

2.1.1. Prototype Greenhouse

The experiment was carried out at the Tibaitatá Research Center of the Colombian Agricultural Research Corporation—AGROSAVIA located in Mosquera Cundinamarca at the geographical coordinates, latitude, 4°41′43.6.6″ N, longitude, 74°12′19.9″ W; and at an altitude of 2545 m above sea level.

A 100 m^2 Venlo-type greenhouse was used, measuring 10 m in both width and in length. The structure has a minimum height of 2.7 m at the facades, rising to a maximum of 5.5 m at the ridge. The roof is made of 2.5 mm thick polycarbonate panels, with a solar radiation transmission coefficient of 87% and a diffusion rate of 90%, as specified by the manufacturer. The lateral sides and facades are covered with translucent glass (Figure 1). The greenhouse is also equipped with various climate control systems, which will be discussed in subsequent sections. The floor is concrete, and inside, masonry planting benches have been installed, each 9 m long, 1 m wide, and positioned 1.2 m above ground level.

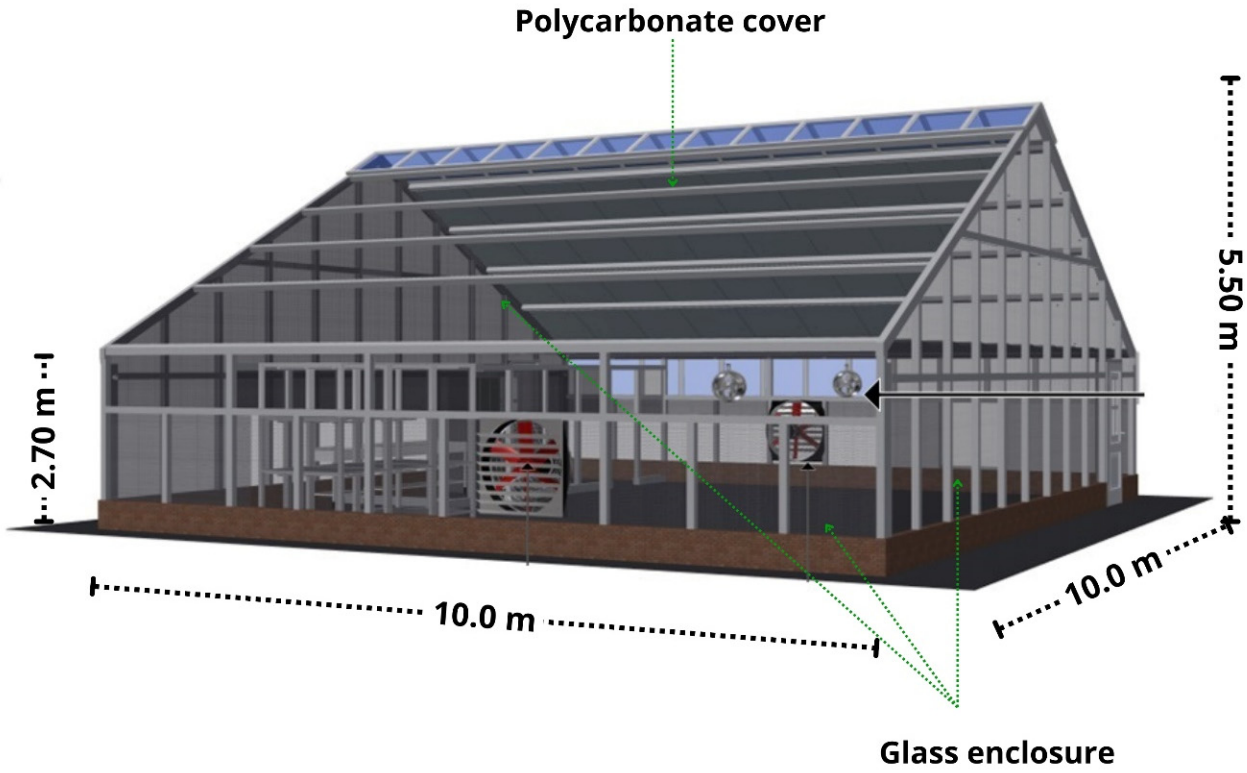

Figure 1. Geometric scheme and some characteristics of the experimental greenhouse.

2.1.2. Central Controller and Sensors for Monitoring and Management

A Hotraco GC-Orion climate controller (https://www.hotraco-horti.com/en/) is centrally located in the greenhouse module. This advanced and versatile controller manages microclimate, irrigation, and fertilization management within greenhouse structures (Figure 2). The system is designed to individually control the microclimates of up to eight distinct compartments, making it ideal for greenhouses with complex environmental requirements. This is particularly advantageous for research greenhouses, where multiple experiments require different controlled conditions within smaller areas. The plug-and-play installation ensures easy setup and provides detailed monitoring of the greenhouse microclimate conditions from any location, improving both operational efficiency and crop growth [40].

Once the central controller is installed, it is operated via computer using the Rainbow+ management software interface (https://www.hotraco-horti.com/en/), integrated into the ORION-GC system. This software enables users to manage and visualize all relevant greenhouse data through graphs and status diagrams. Additionally, with the use of the SmartLink device and the remote+ application, paired with a stable internet network connection, the ORION-GC system can be remotely controlled using a smartphone or tablet. This provides real-time remote access to monitor and manage the greenhouse microclimate from anywhere in the world. The climate control system is further enhanced by monitoring and recording sensors, along with additional controllers located both inside and outside the greenhouse. These sensors record data at one-minute intervals, with the technical specifications summarized in Table 1.

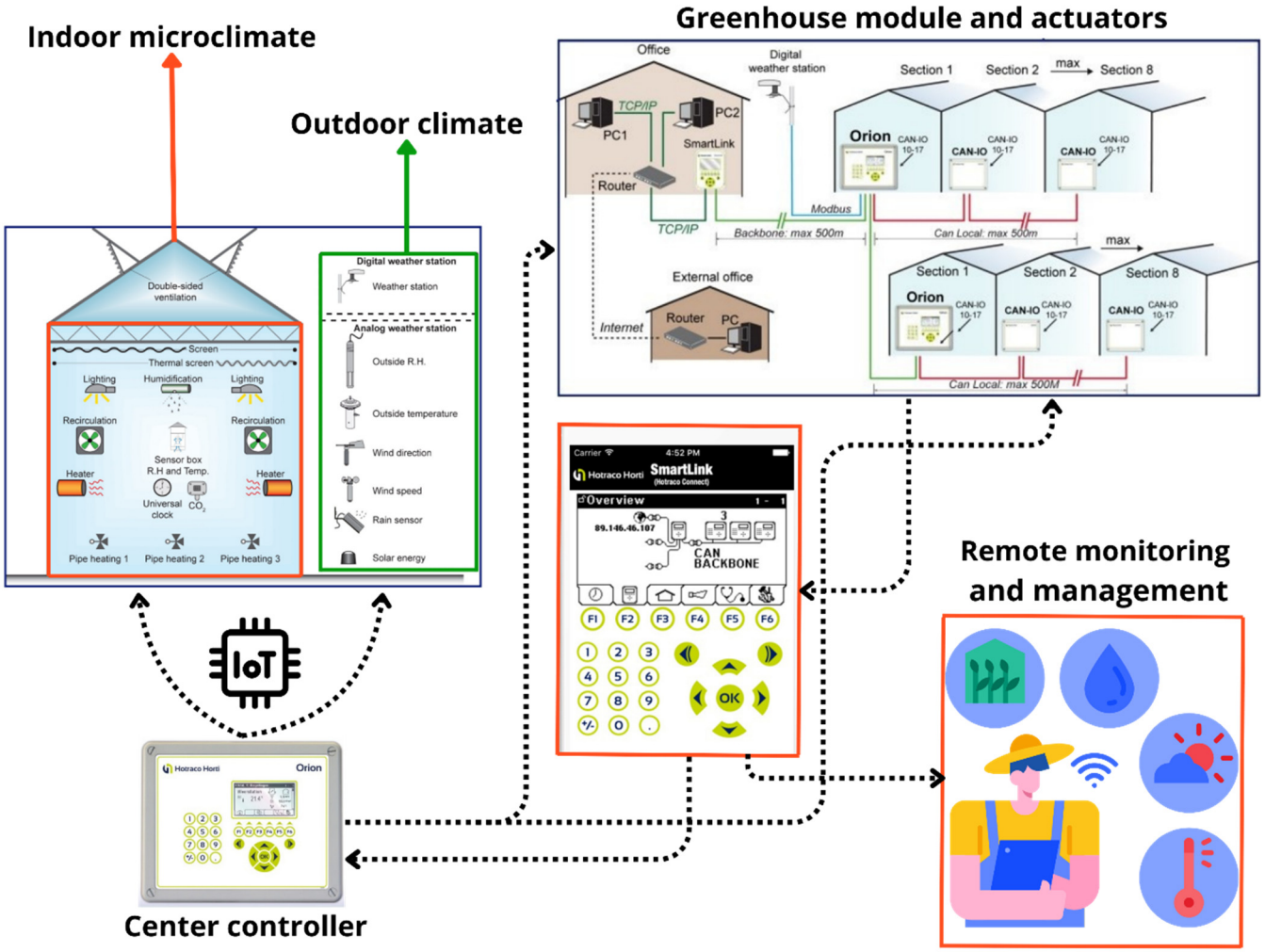

Figure 2. Description of the operation of the remote climate control system.

Table 1. Devices of importance for the climate control system.

Device	Description	Location
CAN IO	CAN IO modules allow more sensors and actuators to be connected to the system, providing comprehensive monitoring and control of the greenhouse environment. The collected data are processed by the main controller to make informed decisions on microclimate control.	Outside of the greenhouse.
External digital weather station, WSC11-Thies	Wind speed: thermal anemometer, measuring range: 0 to 40 ms^{-1}, resolution: 0.1 ms^{-1}, accuracy: 0.1 ms^{-1}. Wind direction: thermal anemometer, measuring range: 1 to 360°, resolution: 1°, accuracy: ±10°. Solar radiation: silicium sensor, measuring range: 1 to 1300 Wm^{-2}, resolution: 1 Wm^{-2}, accuracy: ±10%. Temperature: PT1000, measuring range: −30 to +60 °C, resolution: 0.1 °C, accuracy: ±1 °C. Relative humidity: CMOS capacitive, measuring range: 0 to 100%, resolution: 0.1%, accuracy: ±10%.	Outside of the greenhouse.

Table 1. *Cont.*

Device	Description	Location
SENSOR BOX-ES-24VDC	It collects and transmits crucial micro-climatic data from multiple sensors in a greenhouse, including temperature, humidity, PAR, and CO_2. Sensors are installed in this box and the box is ventilated and radiation-shielded.	Inside of the greenhouse.
Temperature sensor	PT 1000-W. Temperature range: −50 °C to +100 °C, resolution: 0.1 °C, accuracy: ±1 °C.	Inside of the greenhouse.
Relative humidity sensor	RV-A-N probe. measuring range: 0 to 100%, resolution: 1%, accuracy: ±2%.	Inside of the greenhouse.

2.1.3. Microclimate Control Actuators

The experimental greenhouse is equipped with climate control systems to maintain optimal growing conditions, specifically for temperature and relative humidity. It features automatic motorized vents on the sides and ridge, design to open in a butterfly style. These vents provide a ventilation surface of 25 m^2, which is equivalent to 25% of the greenhouse's floor area. In addition, the greenhouse is equipped with a pad cooling system and a fogger system that releases mist at a pressure of 5 bar. Together, these systems help regulate the daytime microclimate to create conditions ideal for the growth and development of the oat crop (Figure 3). The technical specifications of these actuators are summarized in Table 2.

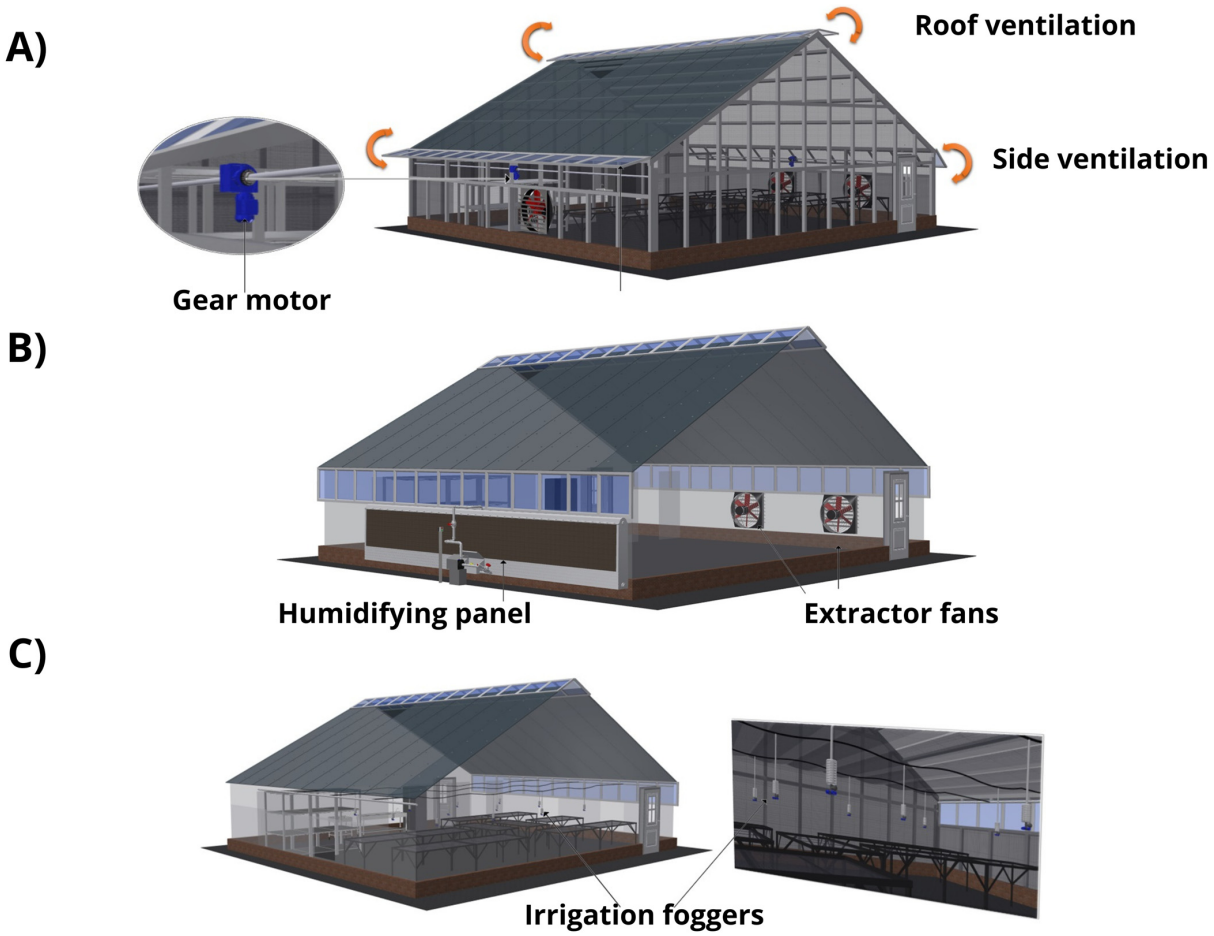

Figure 3. Active climate control strategies installed in the experimental greenhouse. (**A**) automated natural ventilation; (**B**) evaporative cooling equipment; and (**C**) fog cooling.

Regarding microclimate variability and the uniformity of experimental conditions, it is important to highlight that the small size of the greenhouse used in this study minimizes climatic heterogeneity. Unlike larger-scale greenhouses, evaporative cooling systems such as cooling pads demonstrate more efficient air distribution in smaller spaces, significantly reducing temperature and humidity fluctuations. This ensures uniform environmental conditions throughout the experiment [41,42].

Previous research on greenhouses equipped with evaporative cooling systems has shown that optimizing the ratio between cooling pad area and airflow helps maintain climatic homogeneity, even in arid environments. For instance, studies suggest that a cooling pad area of 1 m^2 per 20–30 m^2 of greenhouse space is sufficient to ensure proper humidification and cooling without generating significant microclimate variability. Therefore, given the small and appropriate climate control in this experiment, the impact of microclimatic variability is minimal, ensuring that the experimental conditions remain homogeneous and produce reliable and valid results [43].

Table 2. Technical characteristics of climate control actuators.

Device	Description	Location
Extractor fans	Vostermans of 95 cm diameter and flow rate of 17,300 m^3 h^{-1}, 230 V, 2.7 A and 910 rpm.	Greenhouse facade.
Geared motor with chains and pins	A total of 400 Nm of geared motors for greenhouse ventilation.	Greenhouse ventilation areas
Evaporative cooling pads	CELdek panel—quality 5090—dimensions 9 m wide by 1.2 m high.	Inside of the greenhouse.
Irrigation foggers	NETAFIM COOLNET PRO, nominal flow 5.5 L h^{-1} 4.0 bar pressure—pressure range 3.0–5.0 bar, 4 cross nozzles spaced at 2 m by 2 m.	Inside of the greenhouse.

2.2. High-Throughput Phenotyping Platform

The Plantarray high-throughput gravimetric phenotyping platform, developed by the Israeli company Plant Ditech, was installed in the controlled greenhouse (review [44]). Plantarray is an advanced gravimetric physiological phenotyping platform equipped with multiple sensors. This system enables the rapid and precise selection of plants by providing detailed measurements of key physiological traits that strongly correlate with field performance. The main advantages of this system include its full automation, encompassing experiment control, real-time measurements, and comprehensive data analysis. Plantarray provides consistent, quantitative results, including measurements of the whole plant, from root to shoots, and the surrounding environment (Figure 4). In addition, the system enables precise monitoring of soil and water conditions, as well as the simultaneous management of multiple treatments within the greenhouse. This system continuously evaluates the water flow in the soil–plant–atmosphere complex for each plant, enabling a rapid assessment of yield potential in a dynamic environment [45].

The installed Plantarray system consists of 32 weighing lysimeters, each equipped with independent controllers for irrigation and fertilization, as well as planting containers for the experiment's soil or substrate. The lysimeters are connected to a pressurized irrigation network, which includes a field head with a pressure gauge, pressure regulator, and screen filter. Additionally, the lysimeters employed in this study were calibrated using a range of calibrated weights, typically from 10 g to 10 kg, to ensure high precision in water balance measurements. Studies using similar platforms, such as the PlantDitech PlantArray platform, have shown that lysimeter calibration protocols ensure mass measurement accuracy with uncertainties as low as 3 to 8 g, which is critical for assessing evapotranspiration and water stress [27,44]. Each lysimeter is also equipped with a data transmission and internet cable linked to the main computer, recording gravimetric information every

minute. Additionally, power cables send signals to irrigation controllers according to the experimental programming.

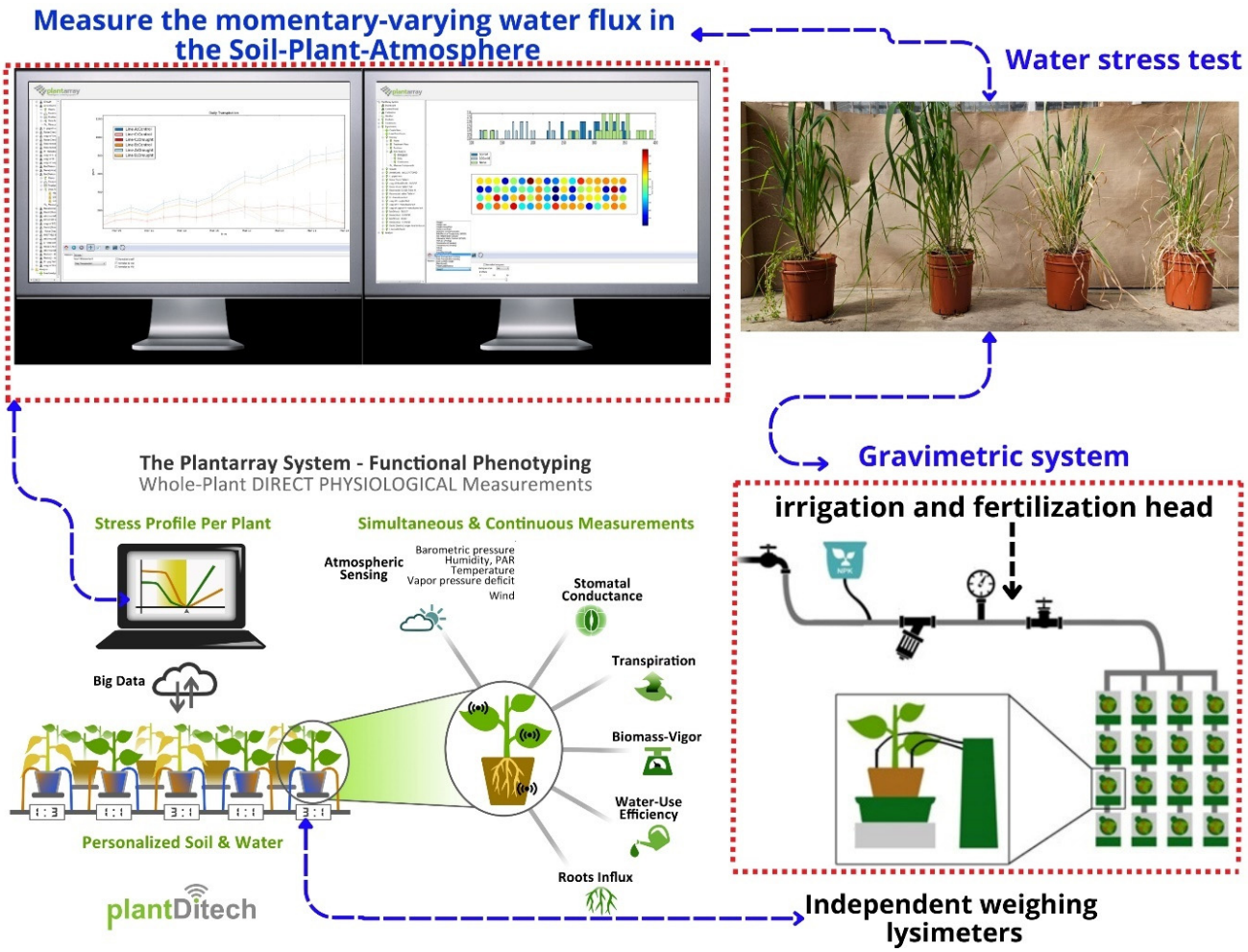

Figure 4. Schematic of the high-throughput phenotyping and big data system.

The system also incorporates a climate station that measures variables such as photosynthetically active radiation (PAR), temperature, relative humidity, and vapor pressure deficit (VPD). The data generated by each experiment can be downloaded and analyzed in real-time via any computer connected to the network, using Plant-DiTech's SPAC analytics platform (www.plant-ditech.com). This setup allows accurate and continuous monitoring of experimental conditions, ensuring effective management and detailed analysis of each essay. A summary of some of the key components of the Plantarray system is given in Table 3.

Table 3. Technical characteristics of the hydraulic and electronic components of the phenotyping platform.

Device	Description	Location
Electric pump	Equipment to always ensure a constant supply of water to the system. The gauge pressure must be guaranteed to remain between 20 and 60 psi.	Irrigation power house.
Irrigation filter	Its function is to filter solid particles that may exist in the water and prevent clogging of irrigation controllers and emitters.	Inside of the greenhouse.

Table 3. *Cont.*

Device	Description	Location
Pressure regulator	Maintains constant water pressure in the irrigation system at 30 psi.	Experimental cultivation bench.
Main valve	Controls the water supply to the irrigation system. In case of malfunction of the irrigation system, it should be shut off.	Experimental cultivation bench.
Plantarray controller	It collects data from the sensors and operates the solenoid valves to form the treatment scenarios in the Plantarray client software. This controller also records and sends data from each experimental unit.	Experimental cultivation bench.
Electronic weighing scales	It consists of a steel structure with a load cell, where its function is to measure changes in biomass and water loss.	Experimental cultivation bench.
Planting platform	It contains the Plantarray, a water reservoir, and a scale assembly. The platform is connected to the Plantarray controller and contains the drippers for irrigation supply.	Experimental cultivation bench.
WatchDog 2475 Plant Growth Station	PAR: measuring range: 0 to 3000 μmolm^{-2} s^{-1}, accuracy: ±5%. Temperature: measuring range: −40 to +125 °C, accuracy: ±0.4 °C. Relative humidity: measuring range: 0 to 100%, accuracy: ±2%. The VPD (kPa) is calculated as a function of the other parameters (temperature and relative humidity).	Experimental cultivation bench.

2.2.1. Plant Material

Seeds of high-Andean forage oat (*Avena sativa* L.) were planted in peat and maintained for 20 days until they reached an average size of 10 cm and five true leaves. Following this step, the seedlings were transplanted into Plantarray phenotyping platform pots containing a mixture of soil and rice husk (3:1) (Figure 5). Soil properties were as follows: pH 6.39, electrical conductivity (0.24 dS m^{-1}), cation exchange capacity (9.60 cmol(+) kg^{-1}), organic matter (19.9 g kg^{-1}), organic carbon (11.5 g kg^{-1}), P (205.247 mg kg^{-1}), S (14.15 mg kg^{-1}), B (0.57 mg kg^{-1}), Ca (5.57 mg kg^{-1}), Mg (1.90 mg kg^{-1}), K (0.36 cmol(+) kg^{-1}), Na (0.05 cmol(+) kg^{-1}), Fe (149.88 mg kg^{-1}), Mn (10.18 mg kg^{-1}), Zn (8.82 mg kg^{-1}), and Cu (6.04 mg kg^{-1}). Once in the pot, foliar fertilizer (Wuxal red top and Wuxal black top) was applied every five days for six weeks to each plant, using a concentration of 1 cm^3 L^{-1}.

2.2.2. Experimental Design

A complete factorial design was established with two factors: water deficit (stress) and inoculation with a microbial consortium (PGPB) made up of the species *Azospirillum brasilense* (strain D7), *Herbaspirillum* sp. (strain AP21), and *Rhizobium leguminosarum* (strain T88). This consortium has demonstrated significant efficacy in mitigating abiotic stress in forage and horticultural crops [46]. Thus, four treatments were established, each duplicated over time, with eight replicates (P-plants) per treatment. The experimental design included the following treatments: (1) irrigated control—Irrigation, (2) water deficit control—Stress, (3) inoculated irrigated—I + PGPB, and 4) inoculated Stress—S + PGPB. PGPB inoculation was performed five days before initiating the drought treatments (Figure 6).

The trial followed a completely randomized block design, alternating treatments of water stress, irrigation, and their combination with IPBG. This arrangement ensures that differences between treatments can be efficiently and comparatively evaluated, minimizing any bias caused by potential environmental gradients within the greenhouse. The linear

arrangement also facilitates monitoring and measurement of critical variables, ensuring appropriate contrasts between treatments under controlled conditions.

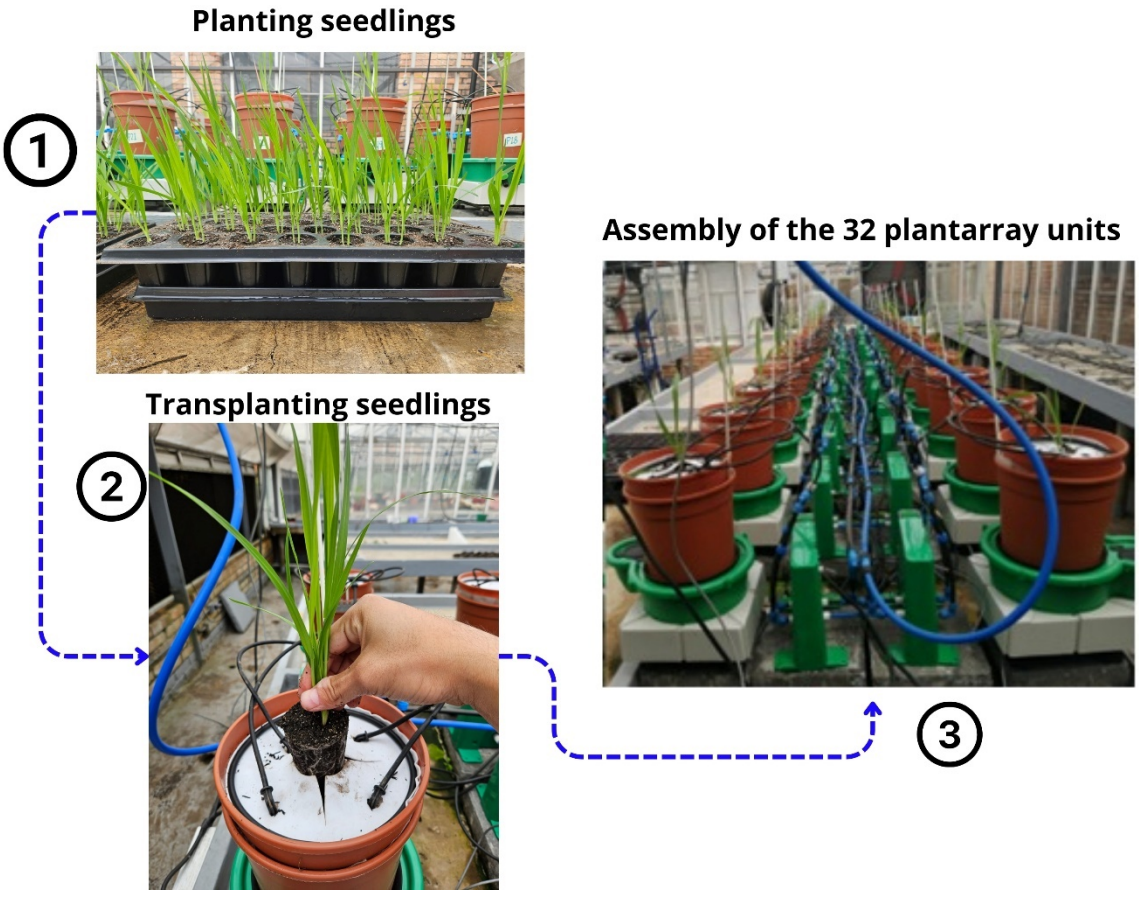

Figure 5. Setup of the experimental trial on the phenotyping platform.

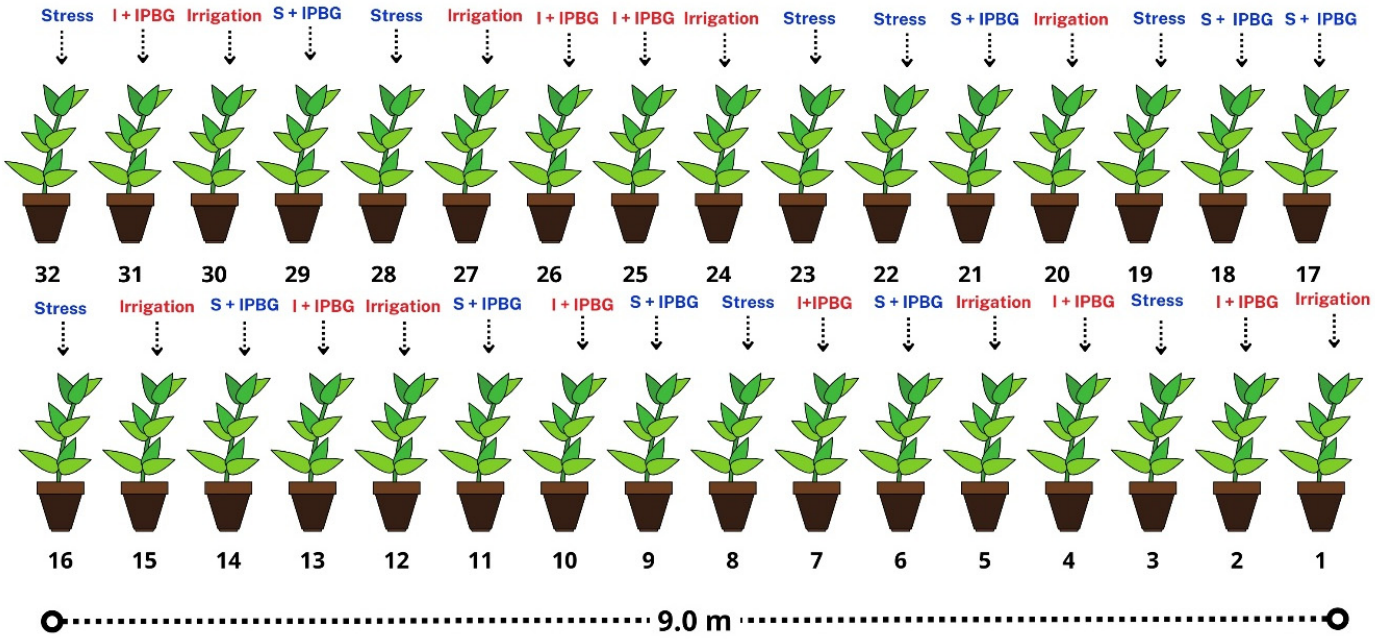

Figure 6. The distribution of the experimental trial in the 32 pots of the physiological phenotyping platform.

The Plantarray platform recorded data for 75 days, from 13 September to 27 November 2023. Initially, a five-day soil drainage test was conducted to ensure the soil drained the applied water pulses adequately, a crucial factor for this type of study [47]. On September 19, oat seedlings were transplanted into the experimental pots. During the first phase, up to 26 October, the 32 beds were irrigated to reach the soil's maximum water storage capacity, applying four nightly irrigation cycles to maintain a consistent gravimetric balance.

Once the plants reached an average daily transpiration of approximately 200 mL, the I + PGPB and S + PGPB treatments were inoculated. Seven days later, drought treatments started, with Stress and S + PGPB plants receiving no irrigation for 15 days. Subsequently, these plants underwent a 5-day recovery phase, with water applied to saturate the soil, followed by a 5-day post-recovery phase. Finally, all plants were removed from the Plantarray platform. This methodological approach follows similar protocols used in previous studies [48,49].

2.3. Parameters Calculated with the Phenotyping Platform

The Plantarray phenotyping platform was used to calculate and record the variables mentioned in the Table 4.

Table 4. Variables measured by the phenotyping platform.

• Variable	• Units
• Daily Transpiration	• (g H_2O)
• Daily Volumetric Water Content	• (cm^3/cm^3)
• Vapor Pressure Deficit (VPD)	• (kPa)
• Photosynthetically Active Radiation (PAR)	• ($\mu mol \cdot m^{-2} \cdot s^{-1}$)

2.4. Determination of Physiological Parameters

2.4.1. Relative Water Content and Biomass

After reaching the physiological point of drought stress and subsequent rehydration, the relative water content (RWC; %) was measured following the method of Cortés-Patiño et al. [34], with some modifications. Leaf segments (10 cm) were weighed for fresh mass (*fw*, g) and placed in ziploc bags with water for 12 h to determine the turgid mass (*tw*, g). Then, the segments were dried in an oven at 70 °C for 48 h to determine the dry mass (*dw*, g). The RWC was calculated using the equation described by Pérez-López et al. [50] (Equation (1)). Stem biomass, root, and total dry biomass (dry biomass; g) were determined after drying the plants in an oven at 70 °C for 48 h.

$$Relative\ water\ content\ (RWC) = \left(\frac{fw - dw}{tw - dw}\right) * 100 \quad (1)$$

2.4.2. Stomatic Conductance and Chlorophyll Fluorescence

Stomatic conductance (g_s, mmol m^{-2} s^{-1}) was measured using a porometer (Decagon Devices Inc., Pullman, WA, USA). Chlorophyll a fluorescence was measured with a modulated fluorometer (MINIPAM-II, Walz, Effeltrich, Germany). The light pulse was applied to leaves, previously adapted to darkness for 20 min, for 1 s at an intensity of 3500 mmol photonsm^{-2} s^{-1}. Measurements were taken between 8:00 am and 10:00 am.

2.4.3. Quantification of Photosynthetic Pigments

The quantification of chlorophyll a (*Chl a*), chlorophyll b (*Chl b*), and total carotenoid content ($x + c$) (mg cm^{-2}), was performed on three-leaf disks per plant in dimethyl sulfoxide (DMSO) [51]. The leaf disks were placed in 1 mL of DMSO and heated in a water bath at

95 °C for 1 h. The extract was then read at 480, 649, and 665 nm using a microplate reader. The pigment content was determined using DMSO equations established by Wellburn [51]:

$$Chl\ a = (12.47\ A_{665.1} - 3.62\ A_{649.1}) \quad (2)$$

$$Chl\ b = 25.06\ A_{649.1} - 6.5\ A_{655.1} \quad (3)$$

$$x + c = (1000\ A_{480} - 1.29_{Chl\ a} - 53.78_{Chl\ b})/220 \quad (4)$$

2.5. Statistical Analysis

Data were analyzed using Prism software (GraphPad, Dotmatics, San Diego, CA, USA) and presented as the mean ± 95% confidence intervals (CI) of eight biological replicates. The normality of residuals was assessed with the Shapiro–Wilk test and visually inspected via Q-Q plots. Homoscedasticity was evaluated using Bartlett's test. When residuals were not normally distributed or variances were not homogeneous (ZAadwvDS < 0.05), the Kruskal–Wallis test was used. If data were normally distributed and variances were homogeneous ($p > 0.05$), ANOVA was applied to determine significant differences between treatments, followed by Tukey's test ($\alpha = 0.05$) for post hoc multiple comparisons. Outliers were identified using the Robust Regression and Outlier Removal (ROUT) method, with a False Discovery Rate (FDR) set at Q = 1%. Different letters indicate significant differences among samples. For significance between two groups, a two-sided Student's *t*-test was used. Significance levels were denoted as * $p \leq 0.05$, ** $p \leq 0.01$, and *** $p \leq 0.001$. All significance analyses were conducted with a 95% confidence interval.

3. Results and Discussion

3.1. External Climatic Conditions

The following is a complete analysis of the temporal behavior of temperature, relative humidity, solar radiation, and wind speed at the experimental site, since these factors directly influence the microclimate generated inside the greenhouses [52,53]. Likewise, crop performance and microclimate control strategies implemented in greenhouses depend to a large extent on these external climatic conditions [54]. This analysis is essential to optimize climate management and improve the energy and environmental efficiency of climate strategies and other factors affecting crop growth and productivity [55,56].

The temporal behavior of the integrated outdoor ambient temperature data set is shown in Figure 7. It is important to note that, due to failures in the electrical infrastructure, there was no internet connection in the greenhouse from 23 September to 27 September, resulting in a data gap. However, the amount of data collected during this measurement period with the recording system is significantly higher than that provided by the public climatology network, which only reports daily averages from a location far from the experimental trial and with delayed reporting. Therefore, it is evident that these IoT stations monitor and record data specific to conditions near the environment of interest, operating autonomously and offering high efficiency in data recording [57].

The data obtained showed clear differences between daytime and nighttime temperatures. The average temperature during the day was 19.4 ± 2.58 °C, while during the night the average was 11.8 ± 1.79 °C. These results indicated that the temperature was generally higher and shows greater variability during the day compared to the night (Figure 7). Additionally, the maximum temperature during the day reached 27.9 °C, while the minimum dropped to 10 °C. On the other hand, during the night, the maximum temperature was 19.7 °C and the minimum was 5.5 °C. These differences between daytime and nighttime temperatures suggest a large thermal amplitude cycle, which may have important implications for greenhouse climate management and other controlled environments, as well as in the development of pests and diseases [58–60].

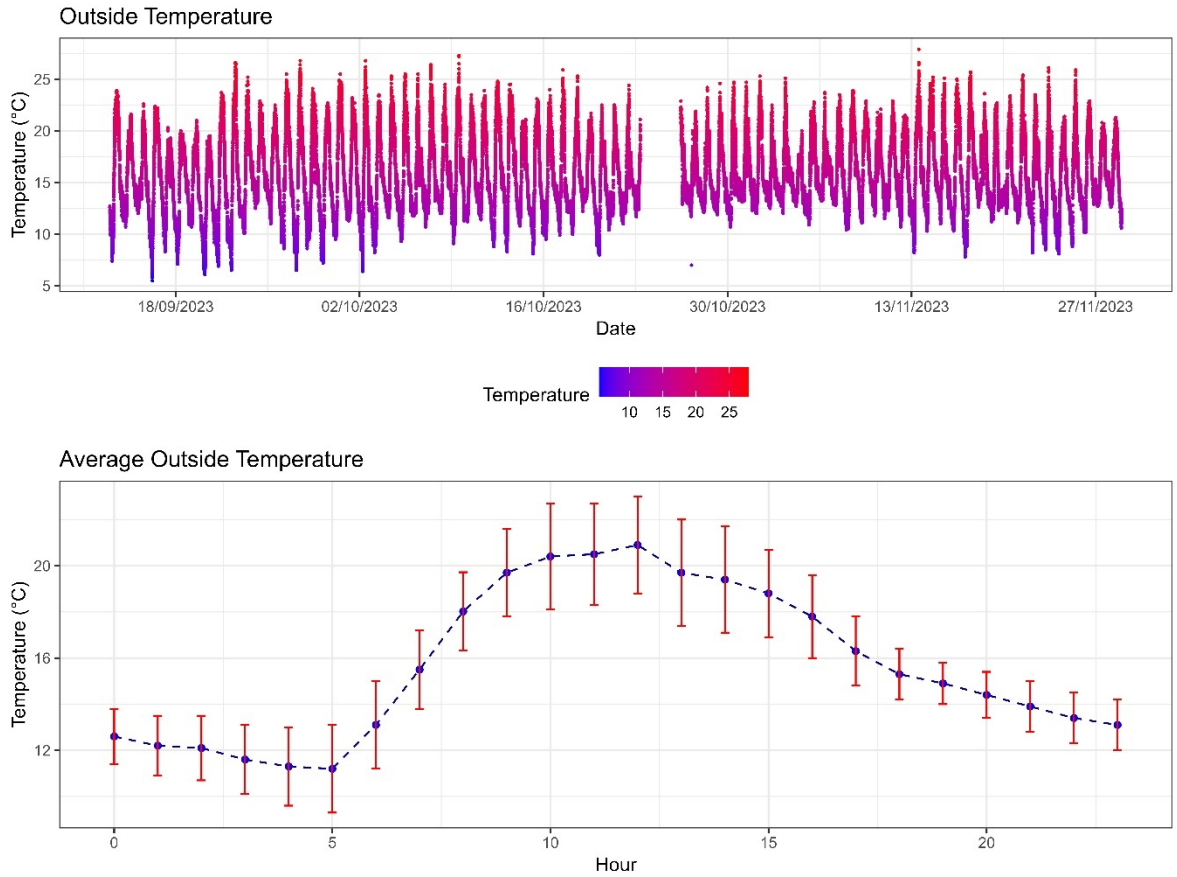

Figure 7. Temporal distribution of outdoor temperature data and hourly mean values during the experimental period.

Regarding relative humidity, the trend observed during the measurement period is illustrated in Figure 8. The relative humidity ranged between 100% saturation during nighttime and lower values close to 40% during the daytime. The data revealed significant differences between day and night humidity levels, which align with previous studies conducted in protected agriculture within the study area [61,62]. The average relative humidity during the day was 67.4 ± 12.1%, while, during the night, it increased to 91.5 ± 7.28%. Furthermore, the extreme values show that the relative humidity reached 100% during both the day and night periods, but the minimum value was notably lower during the day 34% compared to the night 76%. This variability of humidity is influenced by temperature fluctuations and other environmental conditions such as solar radiation [63].

Solar radiation showed a mean value of 301.8 ± 271.3 W/m^2 (Figure 9). These values indicate a high variability in daily solar radiation, which is characteristic for the climatic conditions of the study region. On the other hand, the maximum value of solar radiation was 1310 W/m^2, while the minimum was 0 W/m^2 (at night). This variability in solar radiation influence the microclimate of greenhouses and other agricultural environments, affecting processes such as photosynthesis and evapotranspiration [64]. Understanding these patterns is crucial to optimize microclimate management and improve the energy efficiency of climate control strategies [14,65].

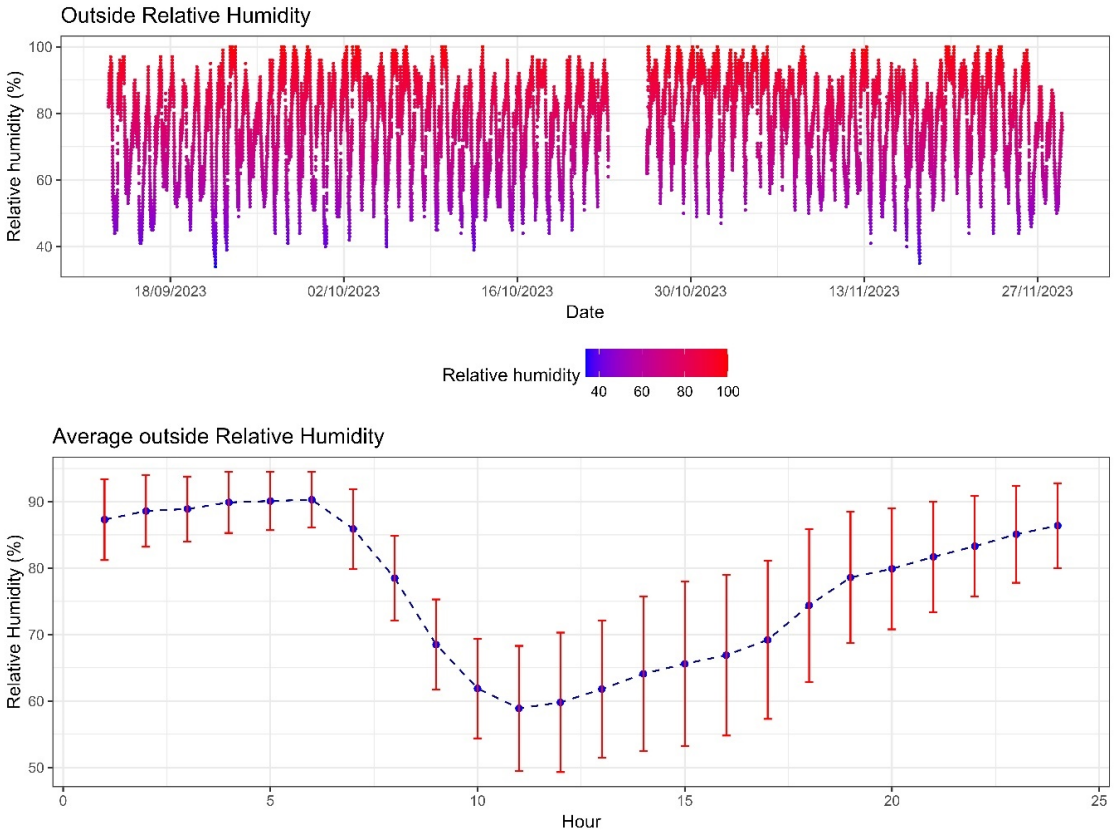

Figure 8. The temporal distribution of outdoor relative humidity data and hourly mean values during the experimental period.

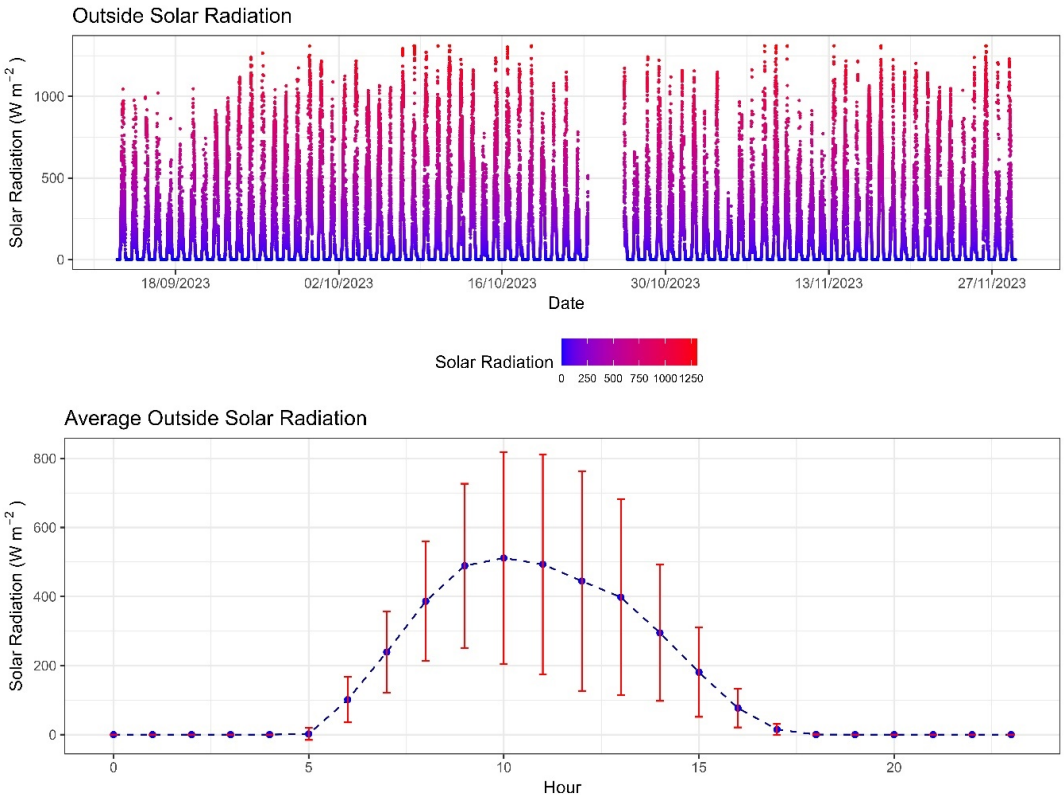

Figure 9. The temporal distribution of solar radiation data and hourly mean values during the experimental period.

Regarding wind speed, the time curve shows that there is a high concentration of data between 0 and 1 ms^{-1} (Figure 10), which is a characteristic behavior of the Bogota savanna [66]. On the other hand, the data showed relevant differences in wind speed between day and night. The average wind speed during the day was 0.886 ± 0.619 m s^{-1}, while during the night it decreased to 0.403 ± 0.318 m s^{-1}. Likewise, the maximum wind speed during the day reached 5.1 m s^{-1}, while the minimum was 0 m s^{-1}. During the night, the maximum wind speed recorded was 2.1 m s^{-1} and the minimum was 0 m s^{-1}. The increased intensity and variability of wind during the daytime can be attributed to climatic factors such as the thermal dynamics of the region, changes in atmospheric pressure, and convection flows [67]. These differences in wind speed are important for greenhouse design and management, as wind influences the distribution of heat, moisture, and carbon dioxide within these structures [68,69].

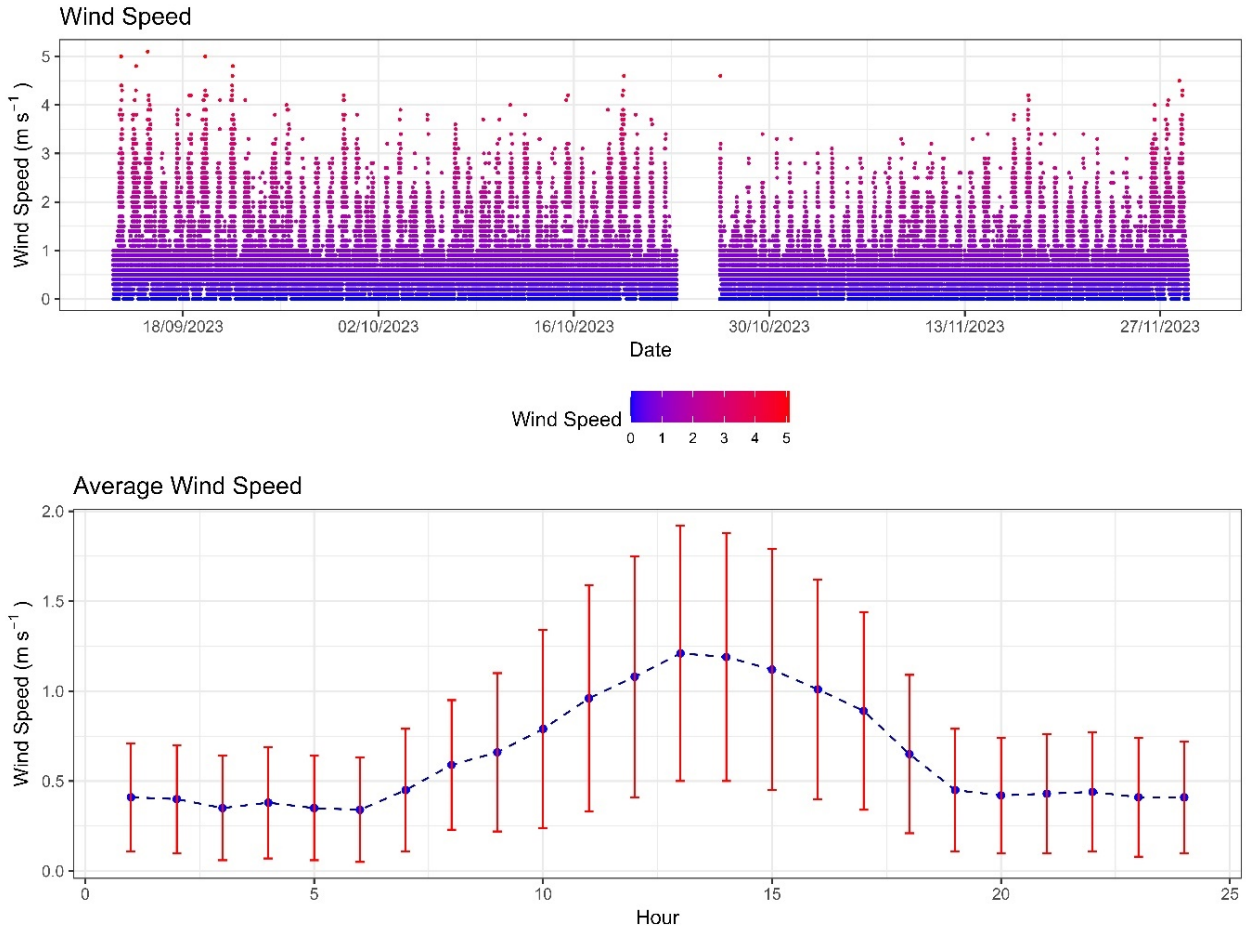

Figure 10. The temporal distribution of wind speed and hourly mean values during the experimental period.

All of the above highlights the importance of proper climate monitoring as it has a significant influence on the microclimatic behavior of greenhouses and other agricultural systems [70].

3.2. Microclimatic Conditions Inside the Greenhouse

The microclimatic conditions inside a greenhouse are crucial for plant development, with temperature and relative humidity significantly influencing plant growth rates [71,72]. In addition, variables such as vapor pressure deficit (VPD) and photosynthetically active radiation (PAR) play essential roles in physiological processes such as transpiration and photosynthesis [73,74]. Therefore, it is essential to conduct a detailed analysis of the behav-

ior of these variables inside the greenhouse used in this research to better understand their impact on the crop and optimize the conditions for adequate plant growth in future trials.

3.2.1. Temperature

In the study, carried out in a greenhouse without night heating but equipped with evaporative cooling and mechanical extractors during the day, some notable differences in thermal behavior during the day and night period were evidenced (Figure 11).

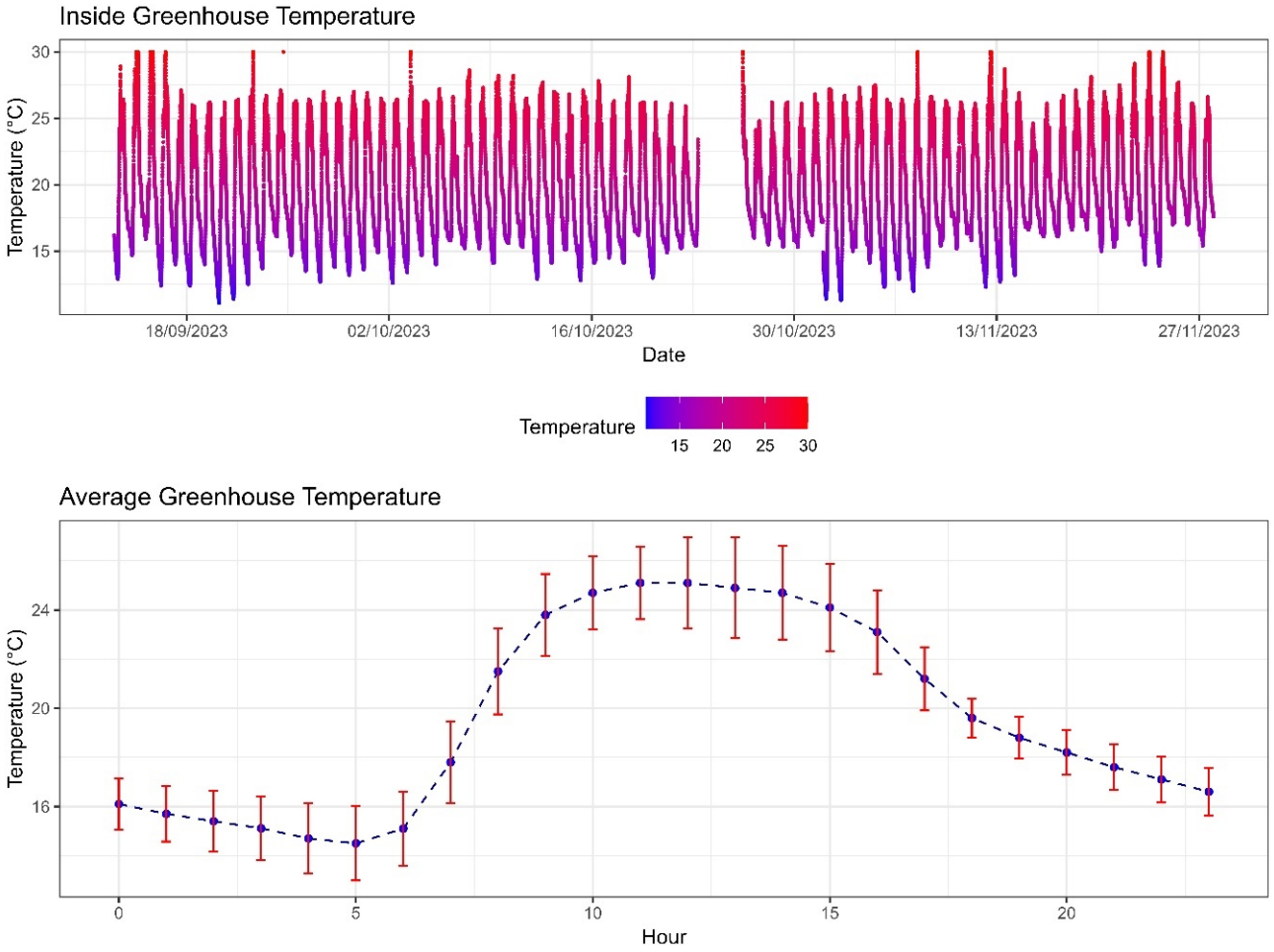

Figure 11. The temporal distribution of temperature and mean hourly values during the experimental period inside the greenhouse.

During daytime hours, the mean temperature was 22.6 ± 3.54 °C, reaching a maximum of 30 °C for several hours during some days (Figure 11). This maximum value was effectively kept below the threshold due to the cooling technology, demonstrating its effectiveness in thermal regulation. On the other hand, during the night, the average temperature dropped to 15.7 ± 1.96 °C with a minimum of 11.1 °C, indicating that there is heat loss inside the structure due to the thermal radiation that leaves the greenhouse to the outside at night and cannot be retained by the polycarbonate cover [75]. These findings show the need to incorporate heating systems to stabilize temperature and optimize growing conditions in the greenhouse [14]. However, the microclimate conditions were adapted to the requirements for the test with high-Andean oats, which were developed for the climatic conditions of the high Andean tropics, where night temperatures can drop to as low as 4 °C [76].

3.2.2. Relative Humidity

The analysis of the relative humidity behavior inside the greenhouse reveals clear patterns related to the day and night cycle of the Bogota Savanna (Figure 12). During the day, the average relative humidity was 57.2 ± 12.4%, reaching a maximum of 89% and a minimum of 28%. These values suggest considerable variability, possibly influenced by greenhouse ventilation, and external climatic conditions such as temperature and solar radiation [61]. In contrast, during the night, the relative humidity increased to an average of 78.8 ± 5.15%, reflecting a maximum of 91% and a minimum of 61%. This increase is attributed to the reduction in temperature, which generates an increase in relative humidity in the atmosphere [77]. Understanding these patterns will be crucial for optimizing growing conditions and effectively managing humidity control systems in the greenhouse for future experiments.

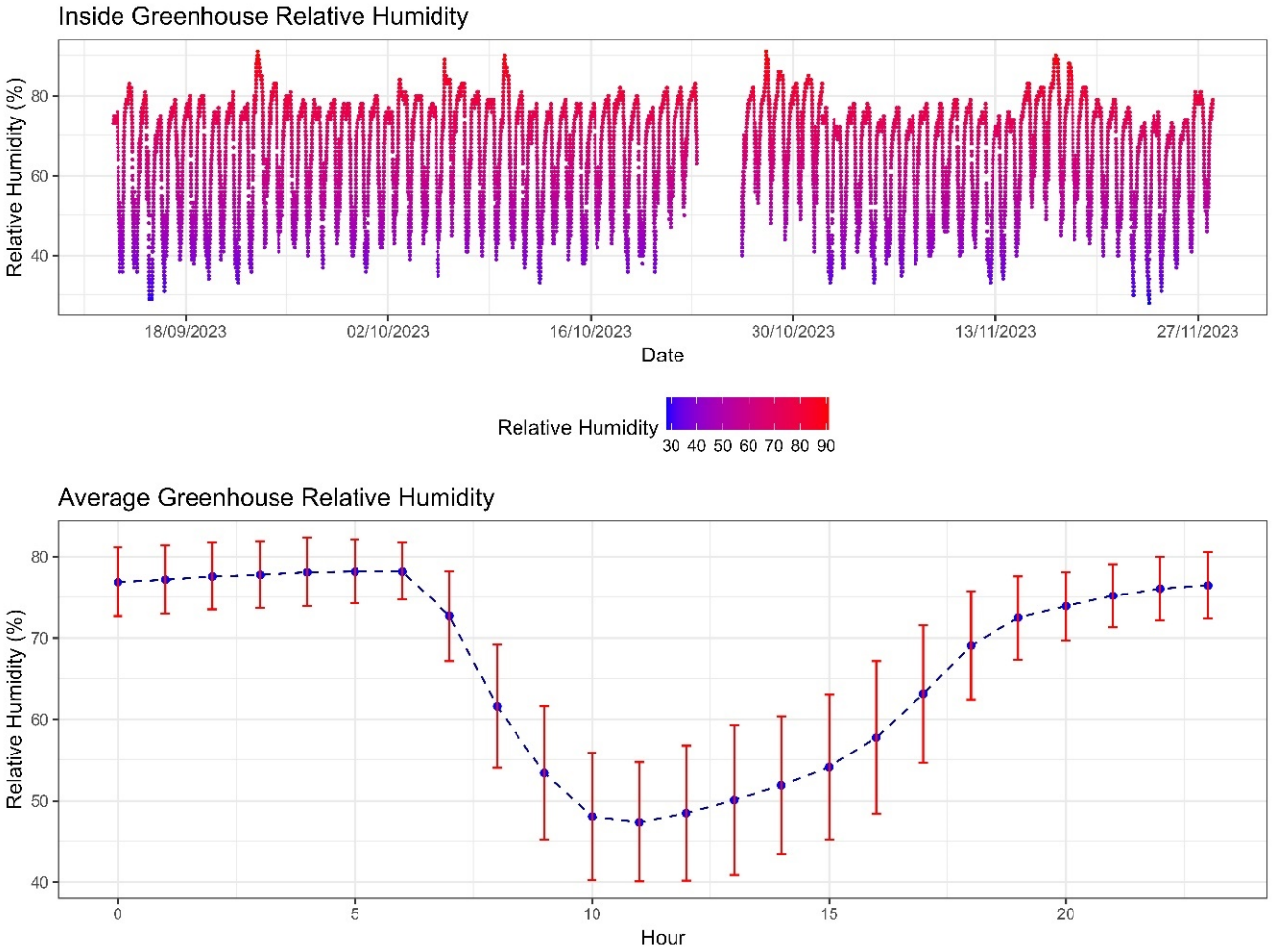

Figure 12. The temporal distribution of relative humidity and mean hourly values during the experimental period inside the greenhouse.

3.2.3. Vapor Pressure Deficit

The analysis of the behavior of the vapor pressure deficit (VPD) demonstrates how variations in internal temperature and relative humidity conditions directly influence this parameter, as it is highly dependent on these variables [78]. During the day, VPD presented a mean of 1.26 ± 0.54 kPa, ranging from a maximum of 3.04 kPa to a minimum of 0.495 kPa (Figure 13). This wide range can be attributed to the intensity of solar radiation that influences greenhouse temperature and plant evapotranspiration. [79]. In contrast, the average VPD at night was 0.46 ± 0.14 kPa, indicating more stable conditions due to the absence of sunlight and a lower photosynthetic activity. The VPD ranged from 0.79 kPa

to 0.259 kPa. These findings show that the nighttime VPD was within an adequate range, as it never fell below 0.2 kPa, which would have increased the risk of foliage diseases [80]. During the day, the average VPD value was in the range of 1.5 kPa, a condition that is optimal for most greenhouse-grown plants, since it promotes a moderate transpiration rate and stomatal conductance without causing excessive water stress [81,82]. However, at some points during the cultivation phase, the VPD reached 2.0 kPa, although it should be noted that since this was a drought stress test, the moisture condition of the greenhouse was low.

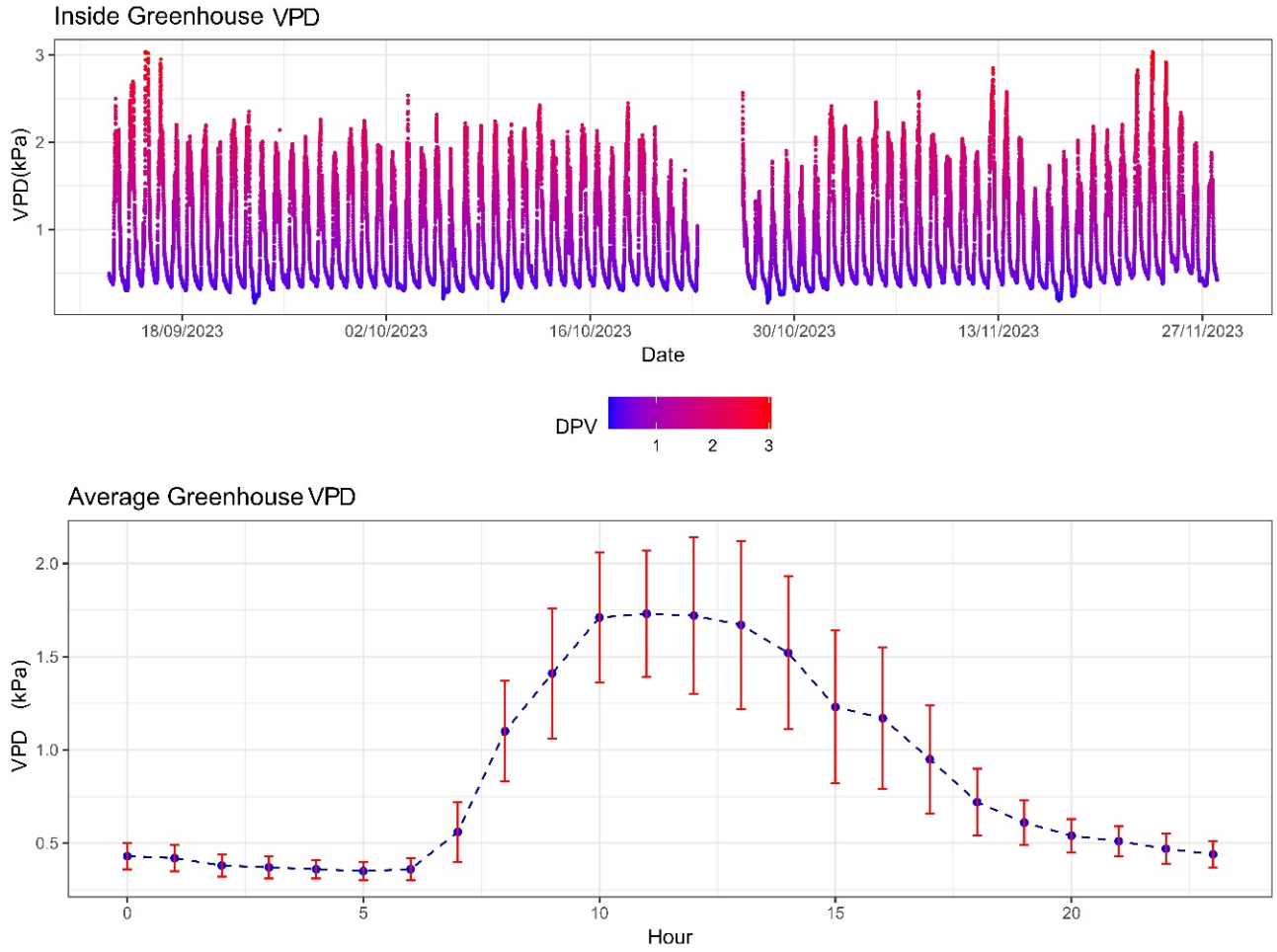

Figure 13. The temporal distribution of the vapor pressure deficit (VPD) and hourly average values during the experimental period inside the greenhouse.

3.2.4. Photosynthetically Active Radiation

Photosynthetically active radiation (PAR) covers wavelengths from 400 to 700 nm and is crucial for photosynthesis, transforming sunlight into energy for plant growth [74]. However, the efficiency in the use of different PAR wavelengths varies due to differences in photon absorption by photosynthetic antenna complexes and the interaction of light with other cellular components that may reflect or absorb it [83]. The analysis of PAR showed an average of 267 $\pm$ 276 µmol m^{-2} s^{-1}, indicating a considerable variability in light intensity throughout the day (Figure 14). Similar PAR behavior was reported for other locations in the department of Cundinamarca [84]. The maximum value was 1788 µmol m^{-2} s^{-1}, highlighting these values at times of high light intensity, between 10:00 and around noon, or at times of direct radiation due to clear skies, which agrees with values reported by [85]. The optimum PAR value required by plants can vary considerably depending on the type of plant and its growth stage. Generally, most greenhouse plants thrive at PAR levels

between 200 and 400 µmol m^{-2} s^{-1} during the active growth phase and may require up to 1050 µmol m^{-2} s^{-1} at other stages of crop development [86].

Therefore, it can be stated that the greenhouse provides adequate light conditions for various crops. It is also important to emphasize that proper PAR management is crucial to optimize photosynthesis and prevent stress or damage caused by excess light exposure in plants. However, in greenhouses without artificial lighting systems, PAR management is primarily limited to maintaining the transparency of the greenhouse canopy, by eliminating dust and other elements that obstruct light transmission and diffusion.

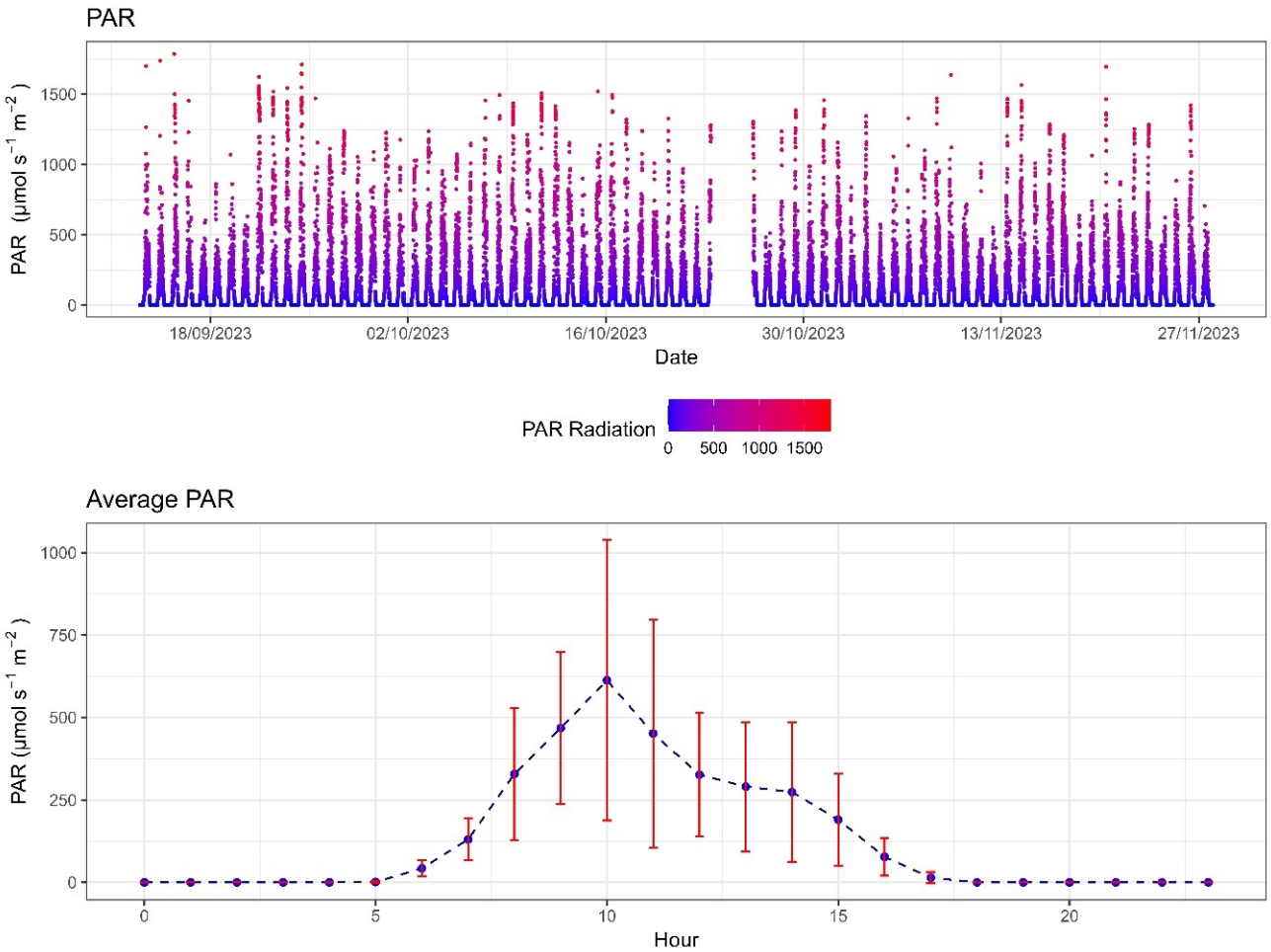

Figure 14. The temporal distribution of PAR and mean hourly values during the experimental period inside the greenhouse.

3.2.5. Differential Thermal Analysis

The thermal differential between the interior of the greenhouse and the external environment showed a mean of 3.9 °C ± 0.9 °C, a maximum of 5.3 °C, and a minimum of 2.0 °C (Figure 15). These data indicate that the greenhouse consistently maintained a higher temperature compared to the outside, which is crucial to promote plant growth under greenhouse conditions [87]. The greenhouse can significantly raise the internal temperature, providing a warmer environment beneficial for plant development, especially during cold nights [88]. Another relevant aspect regarding Colombian greenhouses is that in this experimental greenhouse, no thermal inversion phenomenon was observed. Therefore, there were no negative thermal differentials. This is undoubtedly influenced by the choice of cover material, which provides greater protection against thermal radiation during the night compared to flexible plastic covers [89].

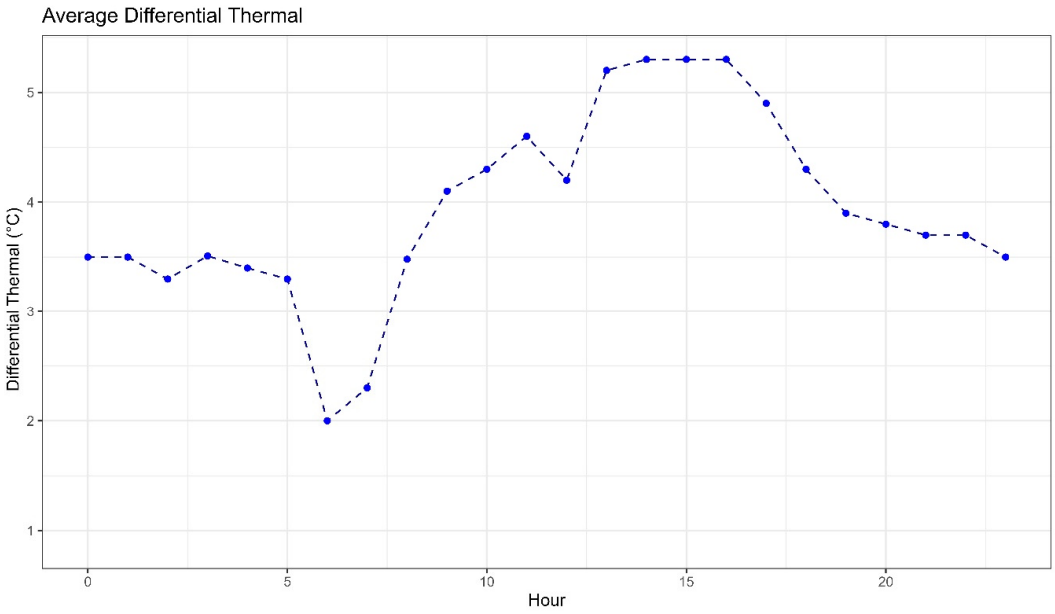

Figure 15. Hourly average values of the thermal differential between the inside and outside environment of the greenhouse.

3.3. Physiological Measurements in Plants

3.3.1. Volumetric Content, Daily Transpiration, Stomatal Conductance, and Relative Water Content of Plants

On day 37, after transplant, the treatments I + PGPB and S + PGPB were inoculated with PGPB consortium, consisting of *Azospirillum brasilense* D7, *Herbaspirillum* sp. AP21, and *Rhizobium leguminosarum* T88. Seven days later, irrigation was suspended for the stress treatments. Consequently, pots began to gradually lose their volumetric water content (VWC) compared to irrigated treatments (Irrigation and I + PGPB) (Figure 16A). Transpiration (Figure 16B) in the Stress and S + PGPB treatments followed the same trend as VWC, with more fluctuations between measurements due to the variability of the greenhouse microenvironment. VWC and transpiration trends were also evidenced in teff and barley plants under drought stress, monitored by a Plantarray lysimeter platform [49,90]. No differences were observed between inoculated and non-inoculated treatments for either variable.

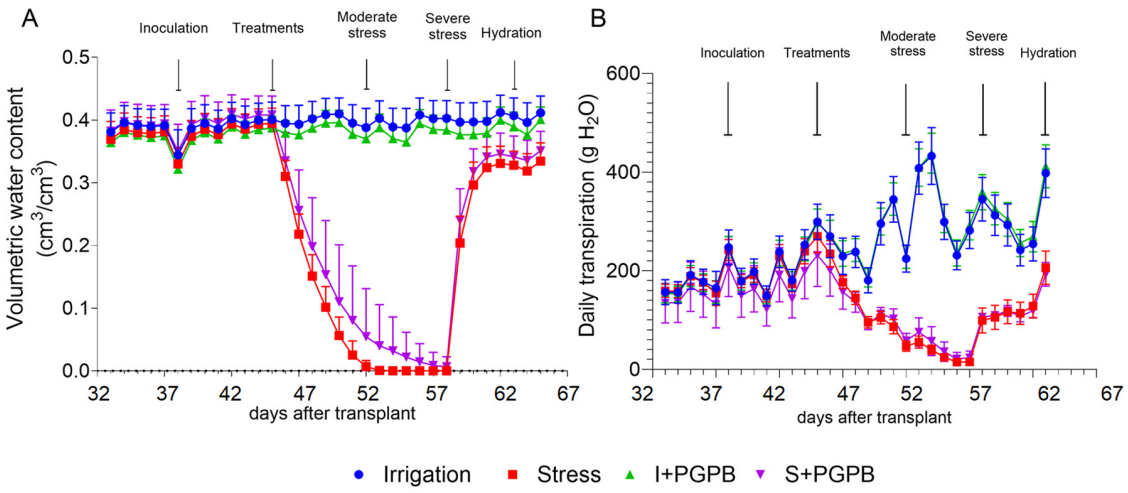

Figure 16. The water balance parameters of oat plants with and without inoculation with a microbial consortium composed of *A. brasilense*, *Herbaspirillum* sp. and *R. leguminosarum* (PGPB), after 17 days of irrigation suspension (Stress), with their respective irrigated controls (Irrigation). (**A**) The volumetric water content and (**B**) the daily plant transpiration.

After nine days of suspending irrigation, the stressed and inoculated plants (S + PGPB) reached moderate stress (Ms) as indicated by their stomatal conductance (g_s) (Figure 17), with values of 142 mmol m^{-2} s^{-1} compared to stressed control plants (Stress), which had values of 70.37 mmol m^{-2} s^{-1}. After five additional days, S + PGPB plants reached values such as those of the Stress treatment under severe stress (Ss). Upon hydration, all plants recovered their water status, as evidenced by increased transpiration (Figure 16B), stomatal conductance g_s (Figure 17), and relative water content (Figure 18). This hydration process highlighted the recovery capacity of the plants treated with the microbial consortium, suggesting a positive effect on the resilience to water stress. [91,92]. It has been documented that plants inoculated with PGPB show increased levels of secondary osmolytes (proline, trehalose, and choline), protective proteins (heat shock proteins—HSPs and late embryogenesis abundant proteins—LEAs), phytohormones (auxins and abscisic acid), and antioxidative enzymes (catalase, ascorbate peroxidase, and glutathione reductase). These increases enhance osmoprotective activity in cells and reduce oxidative stress caused by water deficiency [91,92]. Our results indicate that PGPB inoculation mitigates the negative effects of water deficit stress and facilitates faster and more efficient recovery, promoting improved plant performance under drought conditions and subsequent rehydration.

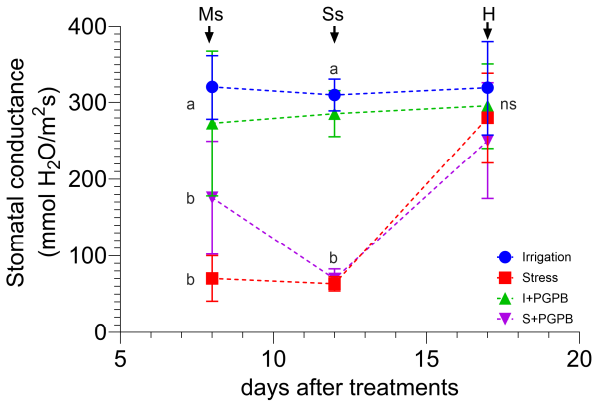

Figure 17. The stomatal conductance of high-Andean oat plants without and with PGPB inoculation under moderate (Ms) and severe (Ss) water deficit stress and five days after hydration (H), with their respective irrigated controls. Data were analyzed using Tukey's test for parametric data and the Kruskal–Wallis test for non-parametric data. Different letters indicate significant differences between treatments ($\alpha = 0.05$).

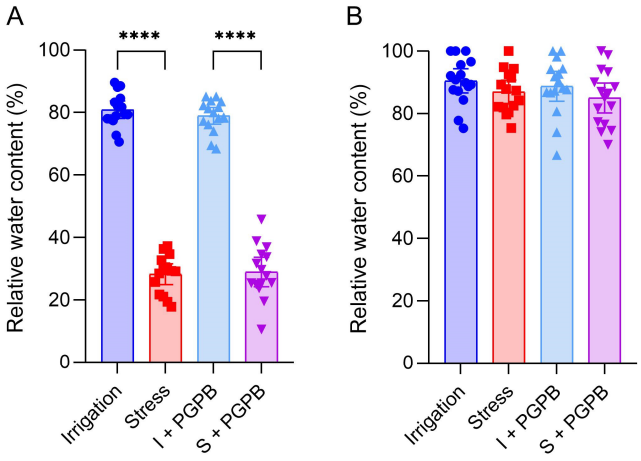

Figure 18. The relative water content (RWC) of high-Andean oat plants without and with PGPB inoculation (**A**) under severe water deficit stress and (**B**) after 5 days following hydration, with their respective irrigated controls. Asterisks indicate significant differences between treatments after a two-sided Student's *t*-test. **** $p \leq 0.0001$.

3.3.2. Biomass, Photosynthetic Pigment Content, and Chlorophyll a Fluorescence

Treatments that were inoculated exhibited greater root growth (Figure 19B), with the irrigated and inoculated treatment (I + PGPB) having the highest total dry biomass (Figure 19C). An increase in growth and biomass production is a response associated with growth promotion. *Azospirillum brasilense, Herbaspirillum* sp., and *Rhizobium leguminosarum* species have demonstrated their ability to produce bioactive compounds, such as indolic compounds and exopolysaccharides, that facilitate stress tolerance and post-stress recovery [93]. Indolic compounds increase cell division and expansion, resulting in larger biomass production. Also, these strains have been evaluated under water stress conditions, showing positive results in plant growth promotion and mitigation of water deficit stress [34,94]. These results suggest that inoculation with the microbial consortium not only favors root growth but also improves the efficiency of water and nutrient uptake, which contributes to an increase in total biomass and even greater efficiency in the use of fertilizers [95].

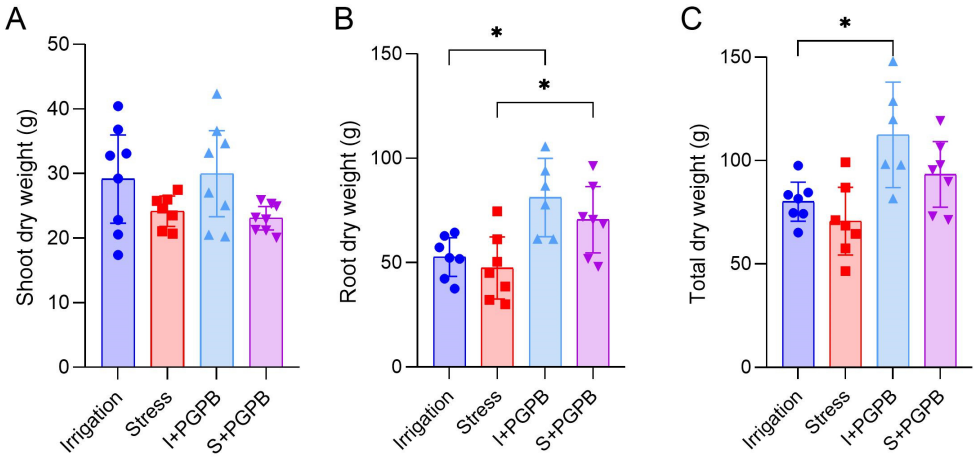

Figure 19. Dry biomass produced by oat plants with and without inoculation with PGPB after 17 days of irrigation suspension, with their respective irrigated controls. (**A**) Shoot dry biomass, (**B**) root dry biomass, and (**C**) total dry biomass. Asterisks indicate significant differences between treatments after a two-sided Student's *t*-test. * $p \leq 0.05$.

Under moderate stress (Ms), differences between irrigation treatments were observed in the non-photochemical quantum yield—Y(NPQ) (Figure 20D). However, under severe stress (Ss) differences were noted in all parameters between stressed and irrigated plants (Figure 20). The increase in the quantum yield of unregulated heat dissipation (Y(NO)) under severe stress indicates stress presence in plants. As stress increases, plants inefficiently regulate energy uptake (increase in Y(NO)), leading to a decrease in non-photochemical quantum yield (Y(NPQ)). This mechanism allows PSII to release excess energy, preventing photodamage [96].

Notably, S + PGPB under Ss obtained similar values of electron transport—ETR and Y(II) as the irrigated control. This suggests that PGPB inoculation may protect the PSII reaction center, reducing the negative impact of water deficit on ETR, as supported by previous findings [97]. Furthermore, the ability of PGPB-treated plants to maintain ETR and Y(II) levels similar to the irrigated control indicates improved tolerance to drought stress. This suggest that the PGPB microbial consortium enhances energy use efficiency under severe stress conditions, maintaining more stable photosynthetic processes [98,99].

Stressed and inoculated plants (S + PGPB), under moderate stress (Ms) had chlorophyll b and carotenoid contents similar to those of the irrigated treatments (Figure 21B,C). This may be related to the effect of the consortium on stress mitigation in oat plants. The stress treatment (Stress) had higher carotenoid content in Ms, indicating that high-Andean oats, under irrigation suspension, tend to accumulate carotenoids in their leaves as a strategy to

avoid photodamage in photosystem II (PSII). Carotenoids dissipate excess light energy and reduce reactive oxygen species production, mitigating photoinhibition [100].

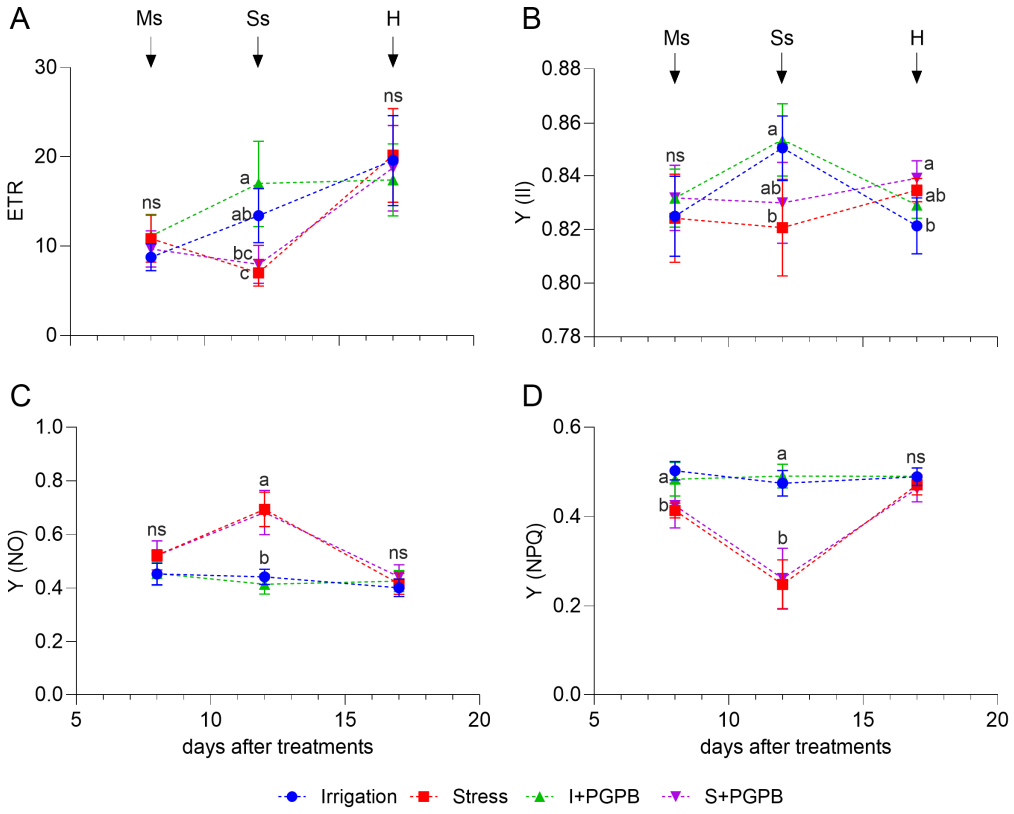

Figure 20. The photochemical and non-photochemical quenching parameters of chlorophyll a fluorescence of high-Andean oat plants with and without PGPB inoculation, under moderate stress (Ms), severe stress (Ss), and after five days of hydration (H) water deficit stress, with their irrigated controls. (**A**) The relative electron transfer rate (ETR); (**B**) the photochemical quantum yield of PSII—Y (II); (**C**) the quantum yield of unregulated heat dissipation—Y (NO); (**D**) the non-photochemical quantum yield—Y (NPQ). Data were analyzed using Tukey's test for parametric data and the Kruskal–Wallis test for non-parametric data. Different letters indicate significant differences between treatments ($\alpha = 0.05$).

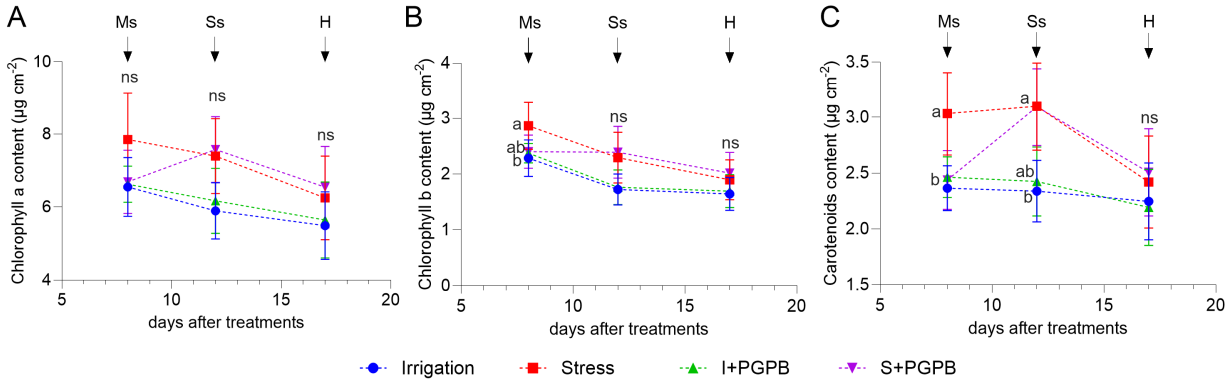

Figure 21. The content of (**A**) chlorophyll a, (**B**) chlorophyll b, and (**C**) carotenoids in high-Andean oat plants inoculated and non-inoculated with the species *A. brasilense*, *Herbaspirillum* sp. and *R. leguminosarum* (PGPB) under moderate water deficit stress (Ms), severe water deficit stress (Ss), and five days after hydration (H). Compared with their respective irrigated controls. Data were analyzed using Tukey's test for parametric data and the Kruskal–Wallis test for non-parametric data. Different letters indicate significant differences between treatments ($\alpha = 0.05$).

This phenomenon was evidenced in the Y(II) results (Figure 20B), where stressed plants maintained values above 0.80 throughout the experiment, indicating the absence of photodamage [101]. During the hydration phase, no significant differences were observed between treatments, consistent with previous physiological variables, such as gs and RWC. This suggests that the microbial consortium not only helps plants to maintain their pigment content under stress conditions but also contributes to rapid recovery after hydration. Therefore, the ability to maintain high carotenoid levels and efficient light energy dissipation may be crucial for stress tolerance and overall plant resilience to adverse conditions.

4. Practical Applications

The findings of this study offer several practical applications that can greatly benefit agricultural producers and promote sustainability in production systems. First, the implementation of IoT-based climate control systems in greenhouses enables the optimization of resource use, such as water and energy, through real-time monitoring and automation of irrigation and ventilation systems. This approach not only improves resource efficiency use but also reduces long-term operational costs. For instance, producers can automatically adjust temperature and humidity conditions to maximize crop growth, thereby reducing losses due to abiotic stress.

Additionally, the use of microbial consortia such as PGPB, not only enhances crop tolerance to drought but also decreases reliance on chemical fertilizers and pesticides. This shift supports more sustainable agricultural practices, leading to crops that are more resilient to climate change and fostering a more stable production system with reduced dependence on external inputs.

Another practical application involves the use of high-throughput phenotyping platforms to accurately monitor plant health and development. This capability allows for more informed and efficient decision-making regarding necessary interventions to maximize crop yield and quality. Furthermore, these tools facilitate the transition to precision agriculture, where producers can optimize the use of each resource in the production process.

5. Conclusions and Recommendations

The implementation of IoT-based climate control systems in greenhouses marks a significant advancement in modern agricultural practices. These systems enable highly accurate monitoring and regulation of essential parameters such as temperature, humidity, and vapor pressure deficit. By leveraging climate control actuators, these systems facilitate precise control, recording, and optimization of the environmental conditions necessary for crop growth, thereby enhancing resource use efficiency. Moreover, the integration of IoT technology in greenhouse environments supports informed decision-making processes and allows for quick adaptation to fluctuating climatic conditions. This ensures stable and reliable microclimatic conditions, particularly crucial for applied research and experimental trials in controlled settings.

Using high-throughput gravimetric phenotyping platforms provided absolute control of irrigation application and accurate data recording of water balance in the plant–soil–atmosphere system. These platforms facilitated the precise acquisition of data on water dynamics, providing a better understanding of the effects of water stress and microbial inoculation on oat plants.

Integrating advanced technologies such as phenotyping platforms, IoT-based climate control systems, and biotechnological tools like microbial consortium inoculation in modern agriculture represents a crucial opportunity to enhance crop resilience to the effects of climate change. These technologies will enable the development of strategies for efficient and precise water resource management, optimizing plant growth and productivity. Consequently, farmers can improve the sustainability of their practices, ensure more stable and high-quality agricultural production, and mitigate the adverse impacts of climate change on food security.

However, one of the main limitations of this study lies in the scale of the experiment, as it was conducted under controlled greenhouse conditions, which may not fully capture the complexity of large-scale agricultural scenarios. Although the effects of water deficit and inoculation with microbial consortia on oats were evaluated, the results need validation across different crops and more variable climatic conditions to generalize the findings. Another limitation is that the monitoring and adjustment of the microclimate were based on IoT sensors and systems, which, despite being accurate, could be affected by technical issues such as connectivity failures or variations in sensor accuracy over the time. Moreover, the potential long-term effects of the continued use of microbial consortia (PGPB) on soil properties were not thoroughly explored, which is essential for ensuring the sustainability of this strategy in future studies.

Future work should focus on larger-scale studies under real agricultural conditions with a greater diversity of crops and environments. Additionally, more advanced IoT technologies could be explored, including systems with backup options for technical failures and increased robustness in connectivity. It would also be valuable to investigate the long-term impact of microbial consortia on soil health, as well as their effectiveness in other crops facing different types of abiotic stress.

Author Contributions: Conceptualization, E.V. and G.A.E.-B.; methodology, E.V., G.T.-T., F.A.V. and G.A.E.-B.; software, E.V., G.T.-T., F.A.V. and G.A.E.-B.; validation, E.V., G.T.-T., F.A.V. and G.A.E.-B.; formal analysis, E.V., G.T.-T., F.A.V. and G.A.E.-B.; investigation, E.V., G.T.-T., F.A.V. and G.A.E.-B.; resources, E.V. and G.A.E.-B.; data curation E.V., G.T.-T. and G.A.E.-B.; writing—original draft preparation, E.V., G.T.-T., F.A.V. and G.A.E.-B.; writing—review and editing, E.V., G.T.-T., F.A.V. and G.A.E.-B.; visualization, E.V., G.T.-T., F.A.V. and G.A.E.-B.; supervision, E.V. and G.A.E.-B.; project administration, E.V.; funding acquisition, E.V. and G.A.E.-B. All authors have read and agreed to the published version of the manuscript.

Funding: This study was financed by the Ministry of Science, Technology and Innovation of Colombia—MINCIENCIAS—through a project called "Fortalecimiento de las capacidades de I + D + i del centro de investigación Tibaitata para la generación, apropiación y divulgación de nuevo conocimiento como estrategia de adaptación al cambio climático en sistemas de producción agrícola ubicados en las zonas agroclimáticas del trópico alto colombiano".

Data Availability Statement: The data are contained in the article.

Acknowledgments: The authors would like to thank the Corporación Colombiana de Investigación Agropecuaria—AGROSAVIA for their technical support in carrying out this research.

Conflicts of Interest: The authors declare no conflicts of interest.

References

1. Gabric, A.J. The Climate Change Crisis: A Review of Its Causes and Possible Responses. *Atmosphere* **2023**, *14*, 1081. [CrossRef]
2. Abd Rabuh, A.; Teeuw, R.M.; Oakey, D.R.; Argyriou, A.V.; Foxley-Marrable, M.; Wilkins, A. Sustainable Geoinformatic Approaches to Insurance for Small-Scale Farmers in Colombia. *Sustainability* **2024**, *16*, 5104. [CrossRef]
3. Klongdee, S.; Netinant, P.; Rukhiran, M. Evaluating the Impact of Controlled Ultraviolet Light Intensities on the Growth of Kale Using IoT-Based Systems. *IoT* **2024**, *5*, 449–477. [CrossRef]
4. de Souza, E.B.; Silva, B.C.S.; Serra, E.M.F.; Ruiz, M.J.B.; Cunha, A.C.; Souza, P.J.P.O.; Pezzi, L.P.; da Rocha, E.J.P.; Sousa, A.M.L.; Silva, J.d.A., Jr. Small Municipalities in the Amazon under the Risk of Future Climate Change. *Climate* **2024**, *12*, 95. [CrossRef]
5. Rugienius, R.; Bendokas, V.; Siksnianas, T.; Stanys, V.; Sasnauskas, A.; Kazanaviciute, V. Characteristics of Fragaria Vesca Yield Parameters and Anthocyanin Accumulation under Water Deficit Stress. *Plants* **2021**, *10*, 557. [CrossRef]
6. Oguz, M.C.; Aycan, M.; Oguz, E.; Poyraz, I.; Yildiz, M. Drought Stress Tolerance in Plants: Interplay of Molecular, Biochemical and Physiological Responses in Important Development Stages. *Physiologia* **2022**, *2*, 180–197. [CrossRef]
7. Hasanuzzaman, M.; Hakim, K.; Nahar, K.; Alharby, H.F. *Plant Abiotic Stress Tolerance*; Bhuyan, M.H.M.B., Hasanuzzaman, M., Nahar, K., Mahmud, J.A., Parvin, K., Bhuiyan, T.F., Fujita, M., Eds.; Springer: Cham, Switzerland, 2019.
8. Tarafdar, M.; Bahadur, V.; Rana, S.; Singh, R.K. A Review: Abiotic Stress on Transpiration, Stomatal Diffusive Resistance and Photosynthetic Rate. *Pharma Innov. J.* **2022**, *11*, 1632–1635.
9. Zia, R.; Nawaz, M.S.; Siddique, M.J.; Hakim, S.; Imran, A. Plant Survival under Drought Stress: Implications, Adaptive Responses, and Integrated Rhizosphere Management Strategy for Stress Mitigation. *Microbiol. Res.* **2021**, *242*, 126626. [CrossRef]

10. Canales, F.J.; Rispail, N.; García-Tejera, O.; Arbona, V.; Pérez-de-Luque, A.; Prats, E. Drought Resistance in Oat Involves ABA-Mediated Modulation of Transpiration and Root Hydraulic Conductivity. *Environ. Exp. Bot.* **2021**, *182*, 104333. [CrossRef]
11. Li, S.-X.; Wang, Z.-H.; Malhi, S.S.; Li, S.-Q.; Gao, Y.-J.; Tian, X.-H. Nutrient and Water Management Effects on Crop Production, and Nutrient and Water Use Efficiency in Dryland Areas of China. *Adv. Agron.* **2009**, *102*, 223–265.
12. Singh, E.; Pratap, A.; Mehta, U.; Azid, S.I. Smart Agriculture Drone for Crop Spraying Using Image-Processing and Machine Learning Techniques: Experimental Validation. *IoT* **2024**, *5*, 250–270. [CrossRef]
13. Maraveas, C.; Bartzanas, T. Application of Internet of Things (IoT) for Optimized Greenhouse Environments. *AgriEngineering* **2021**, *3*, 954–970. [CrossRef]
14. Ortiz, G.A.; Chamorro, A.N.; Acuña-Caita, J.F.; López-Cruz, I.L.; Villagran, E. Calibration and Implementation of a Dynamic Energy Balance Model to Estimate the Temperature in a Plastic-Covered Colombian Greenhouse. *AgriEngineering* **2023**, *5*, 2284–2302. [CrossRef]
15. Rayhana, R.; Xiao, G.; Liu, Z. Internet of Things Empowered Smart Greenhouse Farming. *IEEE J. Radio Freq. Identif.* **2020**, *4*, 195–211. [CrossRef]
16. Lova Raju, K.; Vijayaraghavan, V. IoT Technologies in Agricultural Environment: A Survey. *Wirel. Pers. Commun.* **2020**, *113*, 2415–2446. [CrossRef]
17. Sagheer, A.; Mohammed, M.; Riad, K.; Alhajhoj, M. A Cloud-Based IoT Platform for Precision Control of Soilless Greenhouse Cultivation. *Sensors* **2020**, *21*, 223. [CrossRef]
18. Volosciuc, C.; Bogdan, R.; Blajovan, B.; Stângaciu, C.; Marcu, M. GreenLab, an IoT-Based Small-Scale Smart Greenhouse. *Future Internet* **2024**, *16*, 195. [CrossRef]
19. Khandebharad, R.; Garad, S.; Garad, A.; Moholkar, S.; Daphale, D. IOT-Based Monitoring and Control System for Greenhouses. In Proceedings of the Techno-Societal 2016, International Conference on Advanced Technologies for Societal Applications, Mumbai, India, 9–10 December 2022; Springer: Cham, Switzerland, 2022; pp. 225–232.
20. Shamshiri, R.R.; Bojic, I.; van Henten, E.; Balasundram, S.K.; Dworak, V.; Sultan, M.; Weltzien, C. Model-Based Evaluation of Greenhouse Microclimate Using IoT-Sensor Data Fusion for Energy Efficient Crop Production. *J. Clean. Prod.* **2020**, *263*, 121303. [CrossRef]
21. Nurpilihan, B.; Asmara, S. Application of Internet of Things (IoT) on Microclimate Monitoring System in the ALG Unpad Greenhouse Based on Raspberry Pi. *Tek. Pertan. Lampung* **2022**, *11*, 518–530.
22. Singh, N.; Sharma, A.K.; Sarkar, I.; Prabhu, S.; Chadaga, K. IoT-Based Greenhouse Technologies for Enhanced Crop Production: A Comprehensive Study of Monitoring, Control, and Communication Techniques. *Syst. Sci. Control Eng.* **2024**, *12*, 2306825. [CrossRef]
23. Yuan, H.; Song, M.; Liu, Y.; Xie, Q.; Cao, W.; Zhu, Y.; Ni, J. Field Phenotyping Monitoring Systems for High-Throughput: A Survey of Enabling Technologies, Equipment, and Research Challenges. *Agronomy* **2023**, *13*, 2832. [CrossRef]
24. Bar-On, L.; Zeron, Y.; Sade, N.; Avni, A.; Shacham-Diamand, Y. Examination of Plant Physiological Monitoring Alongside In-Vivo Four-Point-Probe Impedance Spectroscopy of Live Tobacco Plants. In Proceedings of the 2023 IEEE Conference on AgriFood Electronics (CAFE), Torino, Italy, 25–27 September 2023; IEEE: Piscataway, NJ, USA, 2023; pp. 1–4.
25. Chenu, K.; Van Oosterom, E.J.; McLean, G.; Deifel, K.S.; Fletcher, A.; Geetika, G.; Tirfessa, A.; Mace, E.S.; Jordan, D.R.; Sulman, R. Integrating Modelling and Phenotyping Approaches to Identify and Screen Complex Traits: Transpiration Efficiency in Cereals. *J. Exp. Bot.* **2018**, *69*, 3181–3194. [CrossRef] [PubMed]
26. Sun, T.; Cheng, R.; Jiang, R.; Liu, Y.; Sun, Y.; Wang, Z.; Fang, P.; Wu, X.; Ning, K.; Xu, P. Combining Functional Physiological Phenotyping and Simulation Model to Estimate Dynamic Water Use Efficiency and Infer Transpiration Sensitivity Traits. *Eur. J. Agron.* **2023**, *150*, 126955. [CrossRef]
27. Dalal, A.; Shenhar, I.; Bourstein, R.; Mayo, A.; Grunwald, Y.; Averbuch, N.; Attia, Z.; Wallach, R.; Moshelion, M. A Telemetric, Gravimetric Platform for Real-Time Physiological Phenotyping of Plant–Environment Interactions. *JoVE J. Vis. Exp.* **2020**, *162*, e61280.
28. Li, Y.; Wu, X.; Xu, W.; Sun, Y.; Wang, Y.; Li, G.; Xu, P. High-Throughput Physiology-Based Stress Response Phenotyping: Advantages, Applications and Prospective in Horticultural Plants. *Hortic. Plant J.* **2021**, *7*, 181–187. [CrossRef]
29. Illouz-Eliaz, N.; Nissan, I.; Nir, I.; Ramon, U.; Shohat, H.; Weiss, D. Mutations in the Tomato Gibberellin Receptors Suppress Xylem Proliferation and Reduce Water Loss under Water-Deficit Conditions. *J. Exp. Bot.* **2020**, *71*, 3603–3612. [CrossRef]
30. Sacco Botto, C.; Matić, S.; Moine, A.; Chitarra, W.; Nerva, L.; D'Errico, C.; Pagliarani, C.; Noris, E. Tomato Yellow Leaf Curl Sardinia Virus Increases Drought Tolerance of Tomato. *Int. J. Mol. Sci.* **2023**, *24*, 2893. [CrossRef]
31. Uni, D.; Sheffer, E.; Klein, T.; Shem-Tov, R.; Segev, N.; Winters, G. Responses of Two Acacia Species to Drought Suggest Different Water-Use Strategies, Reflecting Their Topographic Distribution. *Front. Plant Sci.* **2023**, *14*, 1154223. [CrossRef]
32. Jaramillo Roman, V.; van de Zedde, R.; Peller, J.; Visser, R.G.F.; van der Linden, C.G.; van Loo, E.N. High-Resolution Analysis of Growth and Transpiration of Quinoa under Saline Conditions. *Front. Plant Sci.* **2021**, *12*, 634311. [CrossRef]
33. Poria, V.; Dębiec-Andrzejewska, K.; Fiodor, A.; Lyzohub, M.; Ajijah, N.; Singh, S.; Pranaw, K. Plant Growth-Promoting Bacteria (PGPB) Integrated Phytotechnology: A Sustainable Approach for Remediation of Marginal Lands. *Front. Plant Sci.* **2022**, *13*, 999866. [CrossRef]

34. Cortés-Patiño, S.; Vargas, C.D.; Alvarez-Flórez, F.; Estrada-Bonilla, G. Co-Inoculation of Plant-Growth-Promoting Bacteria Modulates Physiological and Biochemical Responses of Perennial Ryegrass to Water Deficit. *Plants* **2022**, *11*, 2543. [CrossRef] [PubMed]
35. Vimal, S.R.; Singh, J.S.; Arora, N.K.; Singh, S. Soil-Plant-Microbe Interactions in Stressed Agriculture Management: A Review. *Pedosphere* **2017**, *27*, 177–192. [CrossRef]
36. Naik, K.; Mishra, S.; Srichandan, H.; Singh, P.K.; Sarangi, P.K. Plant Growth Promoting Microbes: Potential Link to Sustainable Agriculture and Environment. *Biocatal. Agric. Biotechnol.* **2019**, *21*, 101326. [CrossRef]
37. Yang, Y.; Guo, Y. Unraveling Salt Stress Signaling in Plants. *J. Integr. Plant Biol.* **2018**, *60*, 796–804. [CrossRef]
38. Chai, Y.N.; Schachtman, D.P. Root Exudates Impact Plant Performance under Abiotic Stress. *Trends Plant Sci.* **2022**, *27*, 80–91. [CrossRef]
39. Akhtar, M.N.; Balodi, R.; Ghatak, A. Microbe-Mediated Mitigation of Plant Stress. In *Microbial Services in Restoration Ecology*; Elsevier: Amsterdam, The Netherlands, 2020; pp. 271–282.
40. Kim, T.; Park, H.; Baek, J.; Kim, M.; Im, D.; Park, H.; Shin, D.; Shin, D. Enhancement for Greenhouse Sustainability Using Tomato Disease Image Classification System Based on Intelligent Complex Controller. *Sustainability* **2023**, *15*, 16220. [CrossRef]
41. Soussi, M.; Chaibi, M.T.; Buchholz, M.; Saghrouni, Z. Comprehensive Review on Climate Control and Cooling Systems in Greenhouses under Hot and Arid Conditions. *Agronomy* **2022**, *12*, 626. [CrossRef]
42. Pardo-Pina, S.; Ferrández-Pastor, J.; Rodríguez, F.; Cámara-Zapata, J.M. Analysis of an Evaporative Cooling Pad Connected to an Air Distribution System of Perforated Polyethylene Tubes in a Greenhouse. *Agronomy* **2024**, *14*, 1187. [CrossRef]
43. Kittas, C.; Katsoulas, N.; Bartzanas, T. Greenhouse Climate Control in Mediterranean Greenhouses. *Cuad. Estud. Agroaliment.* **2012**, *3*, 89–114.
44. Dalal, A.; Shenhar, I.; Bourstein, R.; Mayo, A.; Grunwald, Y.; Averbuch, N.; Attia, Z.; Wallach, R.; Moshelion, M. A High-Throughput Gravimetric Phenotyping Platform for Real-Time Physiological Screening of Plant–Environment Dynamic Responses. *BioRxiv* **2020**, 2001–2020. [CrossRef]
45. Dewi, E.S.; Abdulai, I.; Bracho-Mujica, G.; Appiah, M.; Rötter, R.P. Agronomic and Physiological Traits Response of Three Tropical Sorghum (*Sorghum bicolor* L.) Cultivars to Drought and Salinity. *Agronomy* **2023**, *13*, 2788. [CrossRef]
46. Bejarano-Herrera, W.F.; Marcillo-Paguay, C.A.; Rojas-Tapias, D.F.; Estrada-Bonilla, G.A. Effect of Mineral Fertilization and Microbial Inoculation on Cabbage Yield and Nutrition: A Field Experiment. *Agronomy* **2024**, *14*, 210. [CrossRef]
47. Dalal, A.; Bourstein, R.; Haish, N.; Shenhar, I.; Wallach, R.; Moshelion, M. Dynamic Physiological Phenotyping of Drought-Stressed Pepper Plants Treated with "Productivity-Enhancing" and "Survivability-Enhancing" Biostimulants. *Front. Plant Sci.* **2019**, *10*, 905. [CrossRef] [PubMed]
48. Appiah, M.; Abdulai, I.; Schulman, A.H.; Moshelion, M.; Dewi, E.S.; Daszkowska-Golec, A.; Bracho-Mujica, G.; Rötter, R.P. Drought Response of Water-Conserving and Non-Conserving Spring Barley Cultivars. *Front. Plant Sci.* **2023**, *14*, 1247853. [CrossRef]
49. Paul, M.; Dalal, A.; Jääskeläinen, M.; Moshelion, M.; Schulman, A.H. Precision Phenotyping of a Barley Diversity Set Reveals Distinct Drought Response Strategies. *Front. Plant Sci.* **2024**, *15*, 1393991. [CrossRef]
50. Pérez-López, U.; Robredo, A.; Lacuesta, M.; Muñoz-Rueda, A.; Mena-Petite, A. Atmospheric CO_2 Concentration Influences the Contributions of Osmolyte Accumulation and Cell Wall Elasticity to Salt Tolerance in Barley Cultivars. *J. Plant Physiol.* **2010**, *167*, 15–22. [CrossRef]
51. Wellburn, A.R. The Spectral Determination of Chlorophylls a and b, as Well as Total Carotenoids, Using Various Solvents with Spectrophotometers of Different Resolution. *J. Plant Physiol.* **1994**, *144*, 307–313. [CrossRef]
52. Akrami, M.; Salah, A.H.; Javadi, A.A.; Fath, H.E.S.; Hassanein, M.J.; Farmani, R.; Dibaj, M.; Negm, A. Towards a Sustainable Greenhouse: Review of Trends and Emerging Practices in Analysing Greenhouse Ventilation Requirements to Sustain Maximum Agricultural Yield. *Sustainability* **2020**, *12*, 2794. [CrossRef]
53. Villagrán-Munar, E.A.; Bojacá-Aldana, C.R. CFD Simulation of the Increase of the Roof Ventilation Area in a Traditional Colombian Greenhouse: Effect on Air Flow Patterns and Thermal Behavior. *Int. J. Heat Technol.* **2019**, *37*, 881–892. [CrossRef]
54. Rocha, G.A.O.; Pichimata, M.A.; Villagran, E. Research on the Microclimate of Protected Agriculture Structures Using Numerical Simulation Tools: A Technical and Bibliometric Analysis as a Contribution to the Sustainability of Under-Cover Cropping in Tropical and Subtropical Countries. *Sustainability* **2021**, *13*, 10433. [CrossRef]
55. Chen, T.-H.; Lee, M.-H.; Hsia, I.-W.; Hsu, C.-H.; Yao, M.-H.; Chang, F.-J. Develop a Smart Microclimate Control System for Greenhouses through System Dynamics and Machine Learning Techniques. *Water* **2022**, *14*, 3941. [CrossRef]
56. Bournet, P.E.; Boulard, T. Effect of Ventilator Configuration on the Distributed Climate of Greenhouses: A Review of Experimental and CFD Studies. *Comput. Electron. Agric.* **2010**, *74*, 195–217. [CrossRef]
57. Mitro, N.; Krommyda, M.; Amditis, A. Smart Tags: IoT Sensors for Monitoring the Micro-Climate of Cultural Heritage Monuments. *Appl. Sci.* **2022**, *12*, 2315. [CrossRef]
58. Seginer, I. Sub-Optimal Control of the Greenhouse Environment: Crop Models with and without an Assimilates Buffer. *Biosyst. Eng.* **2022**, *221*, 236–257. [CrossRef]
59. Wang, J.; Lee, W.F.; Ling, P.P. Estimation of Thermal Diffusivity for Greenhouse Soil Temperature Simulation. *Appl. Sci.* **2020**, *10*, 653. [CrossRef]

60. Villagrán-Munar, E.A.; Bojacá-Aldana, C.R. Determinación Del Comportamiento Térmico de Un Invernadero Colgante Colombiano Aplicando Simulación CFD. *Rev. Cienc. Técnicas Agropecu.* **2019**, *28*, 1–11.
61. Villagran, E.; Bojacá, C. Analysis of the Microclimatic Behavior of a Greenhouse Used to Produce Carnation (*Dianthus caryophyllus* L.). *Ornam. Hortic.* **2020**, *26*, 109–204. [CrossRef]
62. Villagrán-Munar, E.A.; Bojacá-Aldana, C.R. Numerical Evaluation of Passive Strategies for Nocturnal Climate Optimization in a Greenhouse Designed for Rose Production (*Rosa* spp.). *Ornam. Hortic.* **2019**, *25*, 351–364. [CrossRef]
63. Garavito, J. El Clima de Bogotá. *Rev. Acad. Colomb. Cienc. Exactas Físicas Nat.* **2020**, *44*, 43–54.
64. Liu, H.; Yin, C.; Hu, X.; Tanny, J.; Tang, X. Microclimate Characteristics and Evapotranspiration Estimates of Cucumber Plants in a Newly Developed Sunken Solar Greenhouse. *Water* **2020**, *12*, 2275. [CrossRef]
65. Gourdo, L.; Fatnassi, H.; Bouharroud, R.; Ezzaeri, K.; Bazgaou, A.; Wifaya, A.; Demrati, H.; Bekkaoui, A.; Aharoune, A.; Poncet, C.; et al. Heating Canarian Greenhouse with a Passive Solar Water–Sleeve System: Effect on Microclimate and Tomato Crop Yield. *Sol. Energy* **2019**, *188*, 1349–1359. [CrossRef]
66. Aragón-Moreno, J.A.; Serna-Castaño, E.D.; Solano-Romero, D.S. Estudio Climatológico de Los Vientos Para La Ciudad de Bogotá En El Periodo 2010–2016. *Entramado* **2019**, *15*, 286–307. [CrossRef]
67. Martinez, O.G.; Noe-Dobrea, I. Agrometeorology in Colombia. In *Agroclimate Information for Development*; Routledge: London, UK, 2022; pp. 269–275.
68. Salinas-Velandia, D.A.; Romero-Perdomo, F.; Numa-Vergel, S.; Villagrán, E.; Donado-Godoy, P.; Galindo-Pacheco, J.R. Insights into Circular Horticulture: Knowledge Diffusion, Resource Circulation, One Health Approach, and Greenhouse Technologies. *Int. J. Environ. Res. Public Health* **2022**, *19*, 12053. [CrossRef] [PubMed]
69. Baeza, E.J.; Pérez-Parra, J.; Montero, J.I. Effect of Ventilator Size on Natural Ventilation in Parral Greenhouse by Means of CFD Simulations. *Acta Hortic.* **2005**, *691*, 465–472. [CrossRef]
70. Peña-Fernández, A.; Colón-Reynoso, M.A.; Mazuela, P. Geometric Analysis of Greenhouse Roofs for Energy Efficiency Optimization and Condensation Drip Reduction. *Agriculture* **2024**, *14*, 216. [CrossRef]
71. Bazgaou, A.; Fatnassi, H.; Bouharroud, R.; Tiskatine, R.; Wifaya, A.; Demrati, H.; Bammou, L.; Aharoune, A.; Bouirden, L. CFD Modeling of the Microclimate in a Greenhouse Using a Rock Bed Thermal Storage Heating System. *Horticulturae* **2023**, *9*, 183. [CrossRef]
72. Vanthoor, B.H.E.; Stanghellini, C.; van Henten, E.J.; de Visser, P.H.B. A Methodology for Model-Based Greenhouse Design: Part 1, a Greenhouse Climate Model for a Broad Range of Designs and Climates. *Biosyst. Eng.* **2011**, *110*, 363–377. [CrossRef]
73. Barreto-Salazar, L.E.; Rochín-Medina, J.J.; Rubio-Astorga, G.J.; Santos-Ballardo, D.U.; Picos-Ponce, J.C. Evaluation of Serrano Pepper Crops Growth under Controlled Conditions of Vapor Pressure Deficit in a Pilot-Scale Hydroponic Greenhouse. *Processes* **2023**, *11*, 3408. [CrossRef]
74. Paskhin, M.O.; Yanykin, D.V.; Gudkov, S. V Current Approaches to Light Conversion for Controlled Environment Agricultural Applications: A Review. *Horticulturae* **2022**, *8*, 885. [CrossRef]
75. Montero, J.I.; Muñoz, P.; Sánchez-Guerrero, M.C.; Medrano, E.; Piscia, D.; Lorenzo, P. Shading Screens for the Improvement of the Night Time Climate of Unheated Greenhouses. *Span. J. Agric. Res.* **2013**, *11*, 32. [CrossRef]
76. Campuzano, L.F.; Rincón, E.C.; Sierra, J.C.; Cuesta, D.T.; Sierra, D.F.N.; Lopez, P.A.P. Altoandina: Nueva Variedad de Avena Forrajera Para La Zona Andina En Colombia. *Agron. Mesoam.* **2020**, *31*, 581–595. [CrossRef]
77. Piscia, D.; Montero, J.I.; Baeza, E.; Bailey, B.J. A CFD Greenhouse Night-Time Condensation Model. *Biosyst. Eng.* **2012**, *111*, 141–154. [CrossRef]
78. Sulman, B.N.; Roman, D.T.; Yi, K.; Wang, L.; Phillips, R.P.; Novick, K.A. High Atmospheric Demand for Water Can Limit Forest Carbon Uptake and Transpiration as Severely as Dry Soil. *Geophys. Res. Lett.* **2016**, *43*, 9686–9695. [CrossRef]
79. Baxevanou, C.; Fidaros, D.; Bartzanas, T.; Kittas, C. Numerical Simulation of Solar Radiation, Air Flow and Temperature Distribution in a Naturally Ventilated Tunnel Greenhouse. *Agric. Eng. Int. CIGR J.* **2010**, *12*, 48–67.
80. Konopacki, P.J.; Treder, W.; Klamkowski, K. Comparison of Vapour Pressure Deficit Patterns during Cucumber Cultivation in a Traditional High PE Tunnel Greenhouse and a Tunnel Greenhouse Equipped with a Heat Accumulator. *Span. J. Agric. Res.* **2018**, *16*, e0201. [CrossRef]
81. McAdam, S.A.M.; Brodribb, T.J. The Evolution of Mechanisms Driving the Stomatal Response to Vapor Pressure Deficit. *Plant Physiol.* **2015**, *167*, 833–843. [CrossRef] [PubMed]
82. Zhang, P.; Yang, X.; Manevski, K.; Li, S.; Wei, Z.; Andersen, M.N.; Liu, F. Physiological and Growth Responses of Potato (*Solanum tuberosum* L.) to Air Temperature and Relative Humidity under Soil Water Deficits. *Plants* **2022**, *11*, 1126. [CrossRef]
83. Inada, K. Action Spectra for Photosynthesis in Higher Plants. *Plant Cell Physiol.* **1976**, *17*, 355–365.
84. Perez Martinez, L.V.; Melgarejo, L.M. Photosynthetic Performance and Leaf Water Potential of Gulupa (Passiflora Edulis Sims, Passifloraceae) in the Reproductive Phase in Three Locations in the Colombian Andes. *Acta Biol. Colomb.* **2015**, *20*, 183–194. [CrossRef]
85. Di Mola, I.; Conti, S.; Bartak, M.; Cozzolino, E.; Ottaiano, L.; Giordano, D.; Melchionna, G.; Mormile, P.; Rippa, M.; Beltrame, L. Greenhouse Photoluminescent PMMA Panels Improve the Agronomical and Physiological Performances of Lettuce (*Lactuca sativa* L.). *Horticulturae* **2022**, *8*, 913. [CrossRef]
86. Chiang, C.; Bånkestad, D.; Hoch, G. Reaching Natural Growth: Light Quality Effects on Plant Performance in Indoor Growth Facilities. *Plants* **2020**, *9*, 1273. [CrossRef] [PubMed]

87. Flores-Velázquez, J.; López-Cruz, I.L.; Mejía-Sáenz, E.; Montero, J.I. Evaluación Del Desempeño Climático de Un Invernadero Baticenital Del Centro de México Mediante Dinámica de Fluidos Computacional (CFD). *Agrociencia* **2014**, *48*, 131–146.
88. Piscia, D.; Montero, J.I.; Bailey, B.; Muñoz, P.; Oliva, A. A New Optimisation Methodology Used to Study the Effect of Cover Properties on Night-Time Greenhouse Climate. *Biosyst. Eng.* **2013**, *116*, 130–143. [CrossRef]
89. Ghani, S.; Bakochristou, F.; ElBialy, E.M.A.A.; Gamaledin, S.M.A.; Rashwan, M.M.; Abdelhalim, A.M.; Ismail, S.M. Design Challenges of Agricultural Greenhouses in Hot and Arid Environments–A Review. *Eng. Agric. Environ. Food* **2019**, *12*, 48–70. [CrossRef]
90. Alemu, M.D.; Barak, V.; Shenhar, I.; Batat, D.; Saranga, Y. Dynamic Physiological Response of Tef to Contrasting Water Availabilities. *Front. Plant Sci.* **2024**, *15*, 1406173. [CrossRef]
91. Cao, M.; Narayanan, M.; Shi, X.; Chen, X.; Li, Z.; Ma, Y. Optimistic Contributions of Plant Growth-Promoting Bacteria for Sustainable Agriculture and Climate Stress Alleviation. *Environ. Res.* **2023**, *217*, 114924. [CrossRef]
92. Vurukonda, S.S.K.P.; Vardharajula, S.; Shrivastava, M.; SkZ, A. Enhancement of Drought Stress Tolerance in Crops by Plant Growth Promoting Rhizobacteria. *Microbiol. Res.* **2016**, *184*, 13–24. [CrossRef]
93. Cortes-Patino, S.; Vargas, C.; Álvarez-Flórez, F.; Bonilla, R.; Estrada-Bonilla, G. Potential of Herbaspirillum and Azospirillum Consortium to Promote Growth of Perennial Ryegrass under Water Deficit. *Microorganisms* **2021**, *9*, 91. [CrossRef]
94. Arruda, B.; Bejarano-Herrera, W.F.; Ortega-Cepeda, M.C.; Campo-Quesada, J.M.; Toro-Tobón, G.; Estrada-Bonilla, G.A.; Silva, A.M.M.; Ferrari Putti, F. Bioinput Inoculation in Common Beans to Mitigate Stresses Caused by a Period of Drought. *Stresses* **2023**, *3*, 842–857. [CrossRef]
95. Chauhan, H.; Bagyaraj, D.J. Inoculation with Selected Microbial Consortia Not Only Enhances Growth and Yield of French Bean but Also Reduces Fertilizer Application under Field Condition. *Sci. Hortic.* **2015**, *197*, 441–446. [CrossRef]
96. Toro-Tobón, G.; Alvarez-Flórez, F.; Mariño-Blanco, H.D.; Melgarejo, L.M. Foliar Functional Traits of Resource Island-Forming Nurse Tree Species from a Semi-Arid Ecosystem of La Guajira, Colombia. *Plants* **2022**, *11*, 1723. [CrossRef] [PubMed]
97. Vishnupradeep, R.; Bruno, L.B.; Taj, Z.; Karthik, C.; Challabathula, D.; Kumar, A.; Freitas, H.; Rajkumar, M. Plant Growth Promoting Bacteria Improve Growth and Phytostabilization Potential of Zea Mays under Chromium and Drought Stress by Altering Photosynthetic and Antioxidant Responses. *Environ. Technol. Innov.* **2022**, *25*, 102154. [CrossRef]
98. Rossi, M.; Borromeo, I.; Capo, C.; Glick, B.R.; Del Gallo, M.; Pietrini, F.; Forni, C. PGPB Improve Photosynthetic Activity and Tolerance to Oxidative Stress in Brassica Napus Grown on Salinized Soils. *Appl. Sci.* **2021**, *11*, 11442. [CrossRef]
99. Abdelaal, K.; AlKahtani, M.; Attia, K.; Hafez, Y.; Király, L.; Künstler, A. The Role of Plant Growth-Promoting Bacteria in Alleviating the Adverse Effects of Drought on Plants. *Biology* **2021**, *10*, 520. [CrossRef] [PubMed]
100. Izuhara, T.; Kaihatsu, I.; Jimbo, H.; Takaichi, S.; Nishiyama, Y. Elevated Levels of Specific Carotenoids during Acclimation to Strong Light Protect the Repair of Photosystem II in *Synechocystis* sp. PCC 6803. *Front. Plant Sci.* **2020**, *11*, 1030. [CrossRef]
101. Maxwell, K.; Johnson, G.N. Chlorophyll Fluorescence—A Practical Guide. *J. Exp. Bot.* **2000**, *51*, 659–668. [CrossRef]

Disclaimer/Publisher's Note: The statements, opinions and data contained in all publications are solely those of the individual author(s) and contributor(s) and not of MDPI and/or the editor(s). MDPI and/or the editor(s) disclaim responsibility for any injury to people or property resulting from any ideas, methods, instructions or products referred to in the content.